Energy Storage Materials 83 (2025) 104756

Contents lists available at ScienceDirect

Energy Storage Materials

journal homepage: www.elsevier.com/locate/ensm

Redefining polymer binders: enabling ion transport and interfacial stability in sulfide-based all-solid-state lithium batteries

Seung-Bo Hong [a,b,1], Young-Jun Lee [b,1], Hun Kim [c], Min Chang Go [a], Un-Hyuck Kim [a,*], Yang-Kook Sun [c,d,*], Dong-Won Kim [b,d,*]

[a] Department of Energy Science and Engineering, Daegu Gyeongbuk Institute of Science and Technology (DGIST), Daegu 42988, South Korea
[b] Department of Chemical Engineering, Hanyang University, Seoul 04763, South Korea
[c] Department of Energy Engineering, Hanyang University, Seoul 04763, South Korea
[d] Department of Battery Engineering, Hanyang University, Seoul 04763, South Korea

ARTICLE INFO

Keywords:
All-solid-state battery
Sulfide solid electrolyte
Polymer binder
Composite electrode
Solid electrolyte sheet

ABSTRACT

Research on sulfide-based all-solid-state lithium batteries (ASSLBs) has predominantly focused on primary components such as active materials, solid electrolytes, and conductive carbons. In contrast, polymer binders have received relatively little attention, despite their critical influence on cell performance. The lack of systematic understanding and rational design strategies for binder materials hinders their effective contribution to the practical development of ASSLBs. While previous studies have primarily emphasized the binders' mechanical integrity and processability, their potential contribution to ionic conductivity and interfacial stability remains largely unexplored. Departing from this traditional focus, this review highlights the essential role of polymer binders in enhancing interfacial adhesion and maintaining continuous Li^+ ion conductive pathways within electrodes and solid electrolyte sheets. Binder design should aim to integrate mechanical robustness with ionic functionality to promote uninterrupted ion transport. From this perspective, polymer binders are redefined as essential design elements that not only provide mechanical cohesion but also compensate for ion transport limitations and stabilize internal interfaces. Their strategic integration at the film level is anticipated to be a decisive factor in advancing ASSLBs technologies.

1. Introduction

The accelerating consumption of fossil fuels in the 21st century has exacerbated climate change, prompting global efforts to transition toward green energy technologies and implement stricter regulations on greenhouse gas emissions [1]. In response, the automotive industry has increasingly shifted from internal combustion engines to electric vehicle (EV) platforms to achieve decarbonization goals [2,3]. However, conventional lithium-ion batteries (LIBs) employing liquid electrolytes face inherent limitations in terms of energy density and safety [4,5]. These challenges have intensified the development of next-generation all-solid-state lithium batteries (ASSLBs) [6]. Among the various solid electrolyte materials, sulfide-based electrolytes (e.g., Li_6PS_5Cl, Li_3PS_4, $Li_{10}GeP_2S_{12}$) have emerged as particularly promising candidates due to their high ionic conductivities at room temperature (~10^{-2} S cm^{-1}), excellent mechanical properties, and favorable processability [7–10]. Over the past years, extensive research has focused on optimizing primary components, including active electrode materials, solid electrolytes, conductive carbons, and polymer binders. Most studies have emphasized morphological control, doping strategies, and surface modifications, typically evaluated at the powder level using torque-cell configurations [11–15]. While these approaches provide valuable insights into the performance of individual components, they fall short in evaluating the practical reliability and integrability essential for the development of viable ASSLBs [16]. Consequently, a research paradigm shift is currently underway, from the material level to the film level, where the focus expands to include structured films or sheets, such as composite electrodes and thin solid electrolytes (Fig. 1). At this stage, the development of polymer binders becomes critical. Polymer binders play an essential role in maintaining interfacial adhesion, accommodating mechanical stress, and preserving Li^+ ion conduction pathways, all of which directly influence the electrochemical performance of ASSLBs

* Corresponding authors.
E-mail addresses: unhyuck.kim@dgist.ac.kr (U.-H. Kim), yksun@hanyang.ac.kr (Y.-K. Sun), dongwonkim@hanyang.ac.kr (D.-W. Kim).
[1] These two authors contributed equally to this work.

https://doi.org/10.1016/j.ensm.2025.104756
Received 18 September 2025; Received in revised form 3 November 2025; Accepted 19 November 2025
Available online 20 November 2025

[17–19]. In addition, the interfacial stability of polymer binders must be ensured to prevent side reactions with solid electrolytes and to achieve long-term cycling stability [20]. It is also noteworthy that, beyond polymer binders, recent studies have reported viscoelastic inorganic glass electrolytes that exhibit polymer-like deformability, inherently maintaining interfacial contact without the need for additional binder phases [21]. In this way, film-level engineering serves as a crucial bridge between material innovation and practical cell integration [22]. It provides a strategic framework for translating accumulated material-level knowledge into viable device architectures. In particular, polymer binders are indispensable for fabricating film-type structures compatible with large-scale pouch cells. However, despite their importance, research on polymer binders remains considerably underexplored compared to studies on other key battery components.

This article aims to assess the current status of polymer binders for the practical development of ASSLBs. In addition, we propose a design strategy that goes beyond conventional approaches by integrating process compatibility with structural control, thereby enabling sustained ion conduction within electrode and solid electrolyte sheets. The discussion is organized according to film-type components, composite cathodes, various types of anodes, and solid electrolyte sheets, with each section evaluating how polymer binders influence cell performance based on representative studies. Through this approach, we aim to establish a film-level binder design strategy tailored for the practical development of ASSLBs, thereby reframing the research agenda and laying the foundation for next-generation all-solid-state battery engineering. In doing so, we redefine polymer binders not merely as mechanical supports or processing aids, but as ion-conductive design elements integral to the functionality of electrode and electrolyte sheets – an aspect that has been largely overlooked in the existing literature,

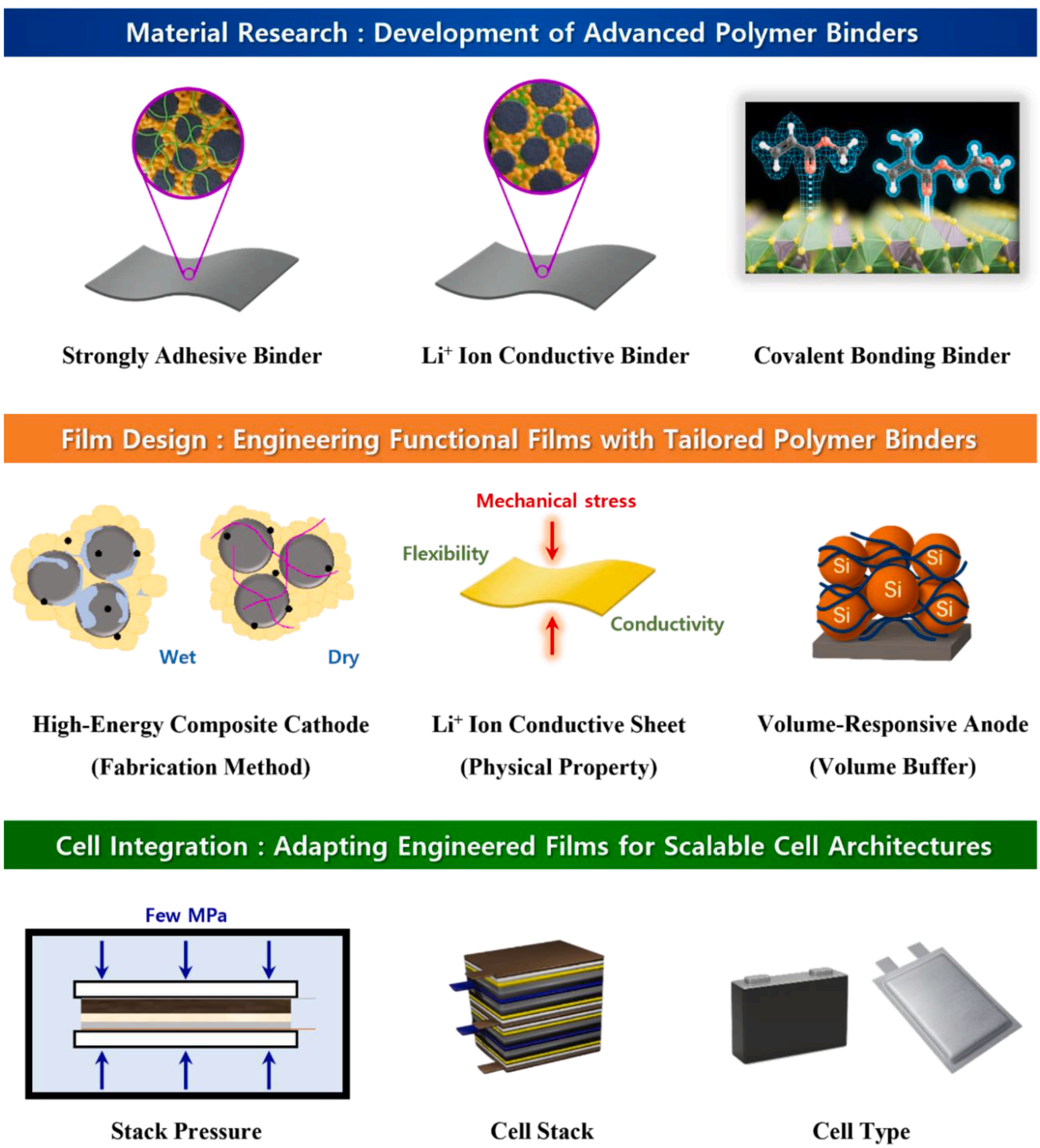

Fig. 1. Schematic overview of material design strategies for sulfide-based ASSLBs. The illustration depicts a development pathway that begins with the engineering of polymer binder materials (top), progresses to the design of films or sheets incorporating tailored binders (middle), and culminates in the integration of these films or sheets into cell architectures for practical battery manufacturing (bottom).

particularly in the context of sulfide-based ASSLBs.

2. Composite cathodes

In ASSLBs, cathode active materials undergo continuous mechanical stress during cycling due to their intrinsic volume changes [23]. Therefore, recent advances in active material design must be taken into account when discussing polymer binders in the context of ASSLBs. Compared to conventional LIB cathodes, cathode active materials for ASSLBs face unique challenges, including particle isolation, interfacial delamination from solid electrolytes, and undesirable interfacial reactions [24]. To address these issues, strategies such as gradient concentration design, morphology engineering of primary particles via high-valence doping, and surface coatings have been explored [25–27]. These approaches have contributed to enhancing the mechanical robustness of cathode active materials and minimizing void formation, thereby supporting the maintenance of continuous Li^+ ion conduction pathways within the composite cathode. Consequently, the design of composite cathode is expected to evolve in parallel with innovations in cathode active materials, with the polymer binder serving as a critical bridge between film-level performance and particle-level engineering. In the composite cathodes for ASSLBs, two key requirements must be fulfilled: (1) the formation of well-defined Li^+ ion conduction pathways, and (2) mechanical stability against stress and volumetric changes. Polymer binders should not be regarded as passive fillers, but rather as functional components that preserve ion conduction pathways, prevent void formation, and stabilize interfacial contacts [28]. However, most studies have primarily focused on their mechanical integrity, often overlooking their critical roles in ionic conduction. These limitations underscore the need for a paradigm shift in redefining the purpose and design of polymer binders. Design strategies must also take into account the constraints imposed by fabrication processes. In dry processes, the absence of organic solvents helps preserve the ionic conductivity of the solid electrolyte but introduces challenges related to binder distribution [29,30]. Therefore, dispersibility and fiber-forming capability become critical design parameters. In contrast, the wet slurry-casting process presents its own challenges, including solid electrolyte degradation and binder migration driven by density gradients during drying [31–33]. These constraints underscore the importance of evaluating polymer binders within a process-specific framework, which is essential for practical implementation. With this in mind, the following section is divided into two main parts, based on design

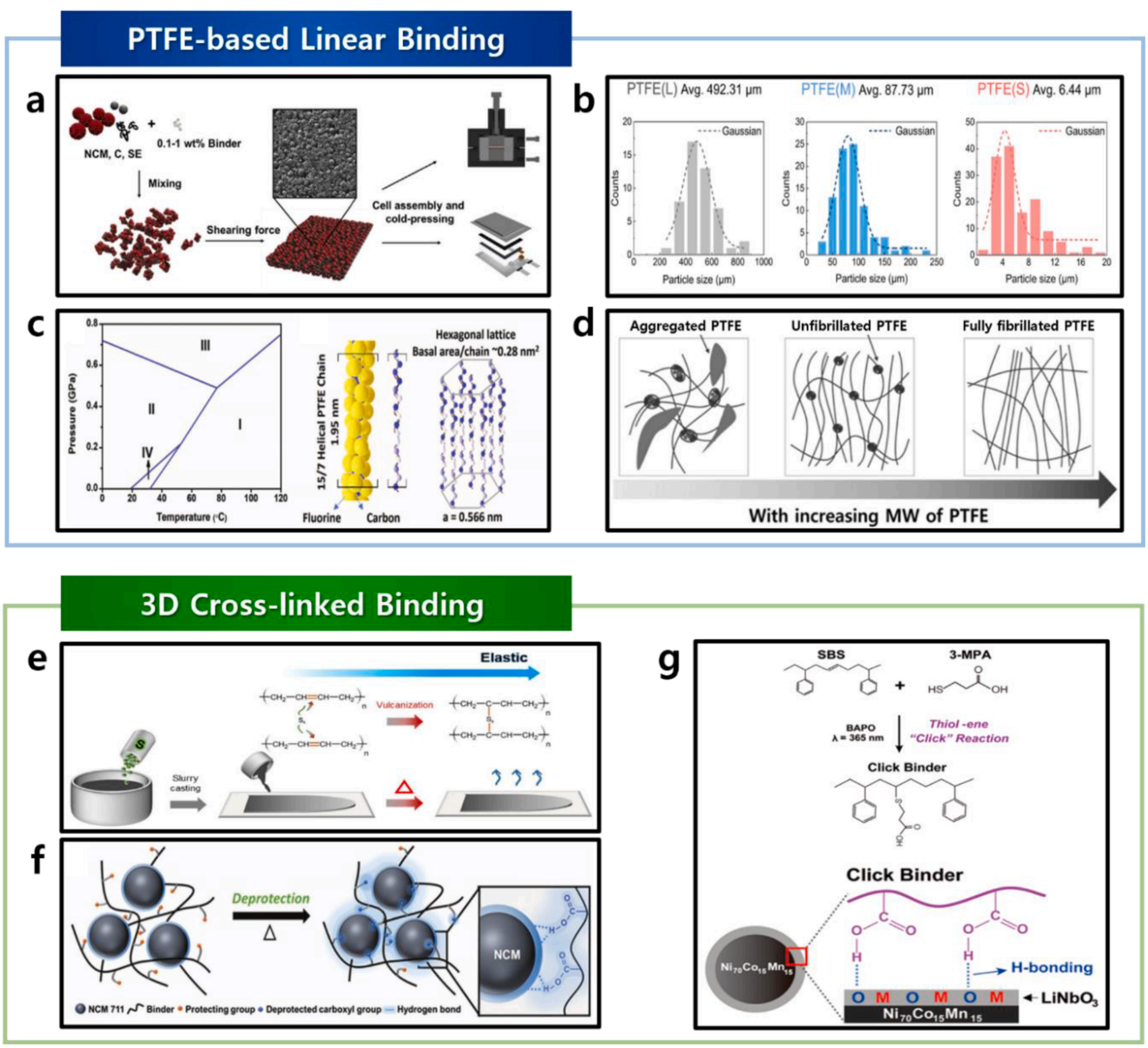

Fig. 2. (a) Fibrous PTFE binder for densification of composite cathodes [37]. Representative optimization strategies for enhancing electrochemical performance through control of PTFE properties: (b) tuning particle size [38], (c) adjusting the degree of crystallinity [39], and (d) controlling molecular weight [40]. Utilization of covalent bonding in binder systems: (e) in-situ vulcanization of butadiene rubber to form 3D-dimensional network [41], (f) deprotection to enable ionic interactions through active functional groups [42], and (g) thiol–ene click reaction for carboxyl functionalization of SBS to improve polarity and dispersion stability [43].

strategies targeting high energy density and high rate capability.

2.1. Binders for high energy density

Enhancing the energy density of ASSLBs can be achieved by increasing the areal capacity through thickening the composite cathodes. However, increasing active material loading alone does not guarantee proportional improvements in cell performance. As the cathode thickness increases, ion transport becomes less efficient due to the disruption of Li^+ ion conduction pathways in thick electrode [34, 35]. To overcome these limitations, several strategies have been explored. Electrode densification reduces film thickness and enhances mechanical contact, while tailored binder systems buffer volume changes and suppress the formation of microcracks. Improving interfacial adhesion among cathode components also contributes to reducing internal resistance. This section highlights representative studies aimed at improving the mechanical integrity and electrochemical performance of thick composite cathodes.

In dry-processed cathodes, polytetrafluoroethylene (PTFE) has been commonly employed to bind cathode components and promote electrode densification [36]. Fraunhofer research group demonstrated that even a minimal amount of PTFE binder was sufficient to ensure both structural integrity and electrochemical performance in dry-processed composite cathodes (Fig. 2**a**) [37]. As a highly crystalline polymer, PTFE undergoes fibrillation under shear force, forming an interconnected fibrous network. These structures not only enhance mechanical integrity but also facilitate the binding of electrode components. Their study highlights how the tunability of binder molecular weight serves as a critical design parameter for morphological control in dry-processed composite cathodes. During the fabrication of free-standing cathode films under applied shear force, insufficient fibrillation can lead to structural defects within the cathode. Subsequent studies have focused on refining cathode architecture by directly modifying and optimizing the PTFE binder. For instance, Lee et al. proposed a strategy to improve the packing density between cathode components and mitigate inhomogeneous contact at the active material – solid electrolyte interface by tuning the particle size of PTFE (Fig. 2**b**) [38]. The use of smaller PTFE particles promoted a more uniform binder distribution within the cathode, resulting in simultaneous improvements in both mechanical strength and ionic conductivity. This study provided experimental evidence that optimizing PTFE binder dispersion can not only address distribution-related limitations in dry-processed electrodes but also minimize electrochemically inactive regions within the composite cathode. The crystallinity of PTFE has emerged as a key parameter governing the mechanical stability of the cathode (Fig. 2**c**) [39]. The physical properties of PTFE vary depending on its degree of crystallinity. Adjusting PTFE crystallinity directly influences its binder function: highly crystalline PTFE enhances mechanical strength, while amorphous domains introduce free volume that facilitates Li^+ ion transport. Thus, tuning the crystallinity of PTFE contributes to both structural stability and ionic conductivity. In addition, recent studies have shown that the molecular weight of PTFE significantly influences its fibrillation behavior. Structural defects in the composite cathode can arise when fibrillation is insufficient under shearing conditions. To address this issue, Lee et al. investigated the molecular weight in which PTFE undergoes adequate fibrillation (Fig. 2**d**) [40]. It was found that high-molecular-weight PTFE, with longer chain lengths and greater chain entanglement, forms more cohesive and uniformly distributed fibrous networks. The thick composite cathodes inevitably undergo significant volume changes, mechanical stress, and interfacial instability during repeated cycling. To effectively address these issues, it is essential to simultaneously tailor the physical properties of PTFE, such as particle size, crystallinity, and molecular weight through molecular design. A summary of PTFE binder properties and their influence on the electrochemical performance of ASSLBs is presented in Table 1.

Despite the fiber network-based binding offered by dry-processing technologies utilizing PTFE, they still face unresolved challenges, particularly with respect to scalability for mass production. To overcome these limitations, wet-slurry casting processes used in conventional LIB electrode fabrication have attracted increasing attention. A unique approach in wet processing involves leveraging the chemical reactivity of polymer binders to form covalent linkages within the cathode structure. Unlike fibrillated PTFE, which primarily relies on the formation of physical networks, these chemically cross-linkable binders enhance interfacial stability and structural integrity by utilizing the inherent chemical functionalities of reactive groups incorporated into the binder structure. For example, in-situ cross-linkable rubber-based binders can initiate vulcanization reactions through the incorporation of sulfur into butadiene rubber (Fig. 2**e**) [41]. This approach is particularly effective under low stack pressure conditions, as it helps preserve the structural integrity of the cathode and suppress void formation during repeated cycling. In this process, sulfur is introduced into the butadiene rubber, triggering cross-linking reactions during the slurry-casting step. By forming polymer networks within the composite cathode, this strategy offers a promising film-level solution to address one of the critical barriers in ASSLBs development. Binders based on deprotection chemistry have also been designed to ensure compatibility with non-polar solvent systems (Fig. 2**f**) [42]. Upon thermal activation during the drying process, these polymers undergo chemical conversion into polar functional groups, thereby enhancing their interfacial affinity with cathode components. A similar concept has been applied to click reaction-enabled binders, in which carboxylic acid groups are introduced into the polymer to promote hydrogen bonding and improve interfacial adhesion (Fig. 2***g***) [43]. To precisely control the degree of functionalization, thiol-ene click chemistry was employed using styrene–butadiene–styrene copolymers. This approach addresses the intrinsic limitations of rubber-based binders by achieving an optimized balance among interfacial adhesion, slurry processability, and ionic conductivity. In addition, leveraging binder functionality has emerged as an effective strategy to address technical challenges in thick

Table 1
Summary of the molecular design parameters affecting the performance of PTFE-based dry-processed composite cathodes.

Design parameter	Property	Cathode active material	Active material loading (mg cm^{-2})	Cell performance: Initial discharge capacity (mAh g^{-1})	Cell performance: Capacity retention (% @ n cycle)	Ref.
Particle size	492.3 μm	$LiNi_{0.8}Co_{0.15}Al_{0.05}O_2$	15	165.7 @ 0.2 C	65.7 % @ 100	[38]
	87.73 μm			182.3 @ 0.2 C	85.1 % @ 100	
	6.44 μm			188.7 @ 0.2 C	90.4 % @ 100	
Crystallinity	18.8 %	$LiNi_{0.8}Co_{0.1}Mn_{0.1}O_2$	20	162 @ 0.1 C *	64.1 % @ 200	[39]
	41.3 %			165 @ 0.1 C *	69.6 % @ 200	
	88.1 %			167 @ 0.1 C *	84.1 % @ 200	
Molecular weight	1.2×10^6 g mol^{-1}	$LiNi_{0.82}Co_{0.10}Mn_{0.08}O_2$	22.5	121.8 @ 0.5 C	83.5 % @ 300	[40]
	1.8×10^6 g mol^{-1}			135.2 @ 0.5 C	89.3 % @ 300	
	3.2×10^6 g mol^{-1}			144.2 @ 0.5 C	97.4 % @ 300	

* Data were obtained from published figures because exact numerical values were not available.

composite cathodes for high energy density, particularly mechanical degradation caused by the gradual accumulation of particle cracks during repeated cycling. In liquid electrolyte-based LIBs, such cracks remain electrochemically active due to the infiltration of the liquid electrolyte, which maintains Li^+ ion accessibility. In contrast, the formation of microcracks in ASSLBs can disconnect active materials from the ion conduction network, resulting in electrochemically inactive or "dead" particles [44]. Given the rigid ion conduction framework of ASSLBs, mitigating crack propagation in active materials has become a critical engineering priority. To address this issue, recent studies have incorporated stress-relieving and crack-healing additives into composite cathodes. Kim et al. demonstrated that the introduction of $LiPO_2F_2$ into dry-processed cathode effectively reduced mechanical stress at the interface between the active material and the solid electrolyte, while promoting cathode densification [45]. Owing to its fine and narrowly distributed particle size, the additive enabled uniform stress transfer and facilitated bimodal particle packing, thereby improving both structural cohesion and ionic conductivity. Furthermore, upon decomposition on the active material surface, $LiPO_2F_2$ formed a protective layer that mitigated the oxidative degradation of Li_6PS_5Cl, resulting in enhanced cycling stability. Lee et al. demonstrated that a nitrile butadiene rubber (NBR) binder used in wet-processed cathodes exhibited self-healing behavior over extended cycling [46]. Their study showed that cathode electrolyte interphase-forming species gradually filled microcracks formed under mechanical stress, effectively restoring Li^+ ion conduction pathways and reducing interfacial resistance. This report suggests that binders can function not only as mechanical frameworks but also as dynamic matrices that accommodate decomposition products and

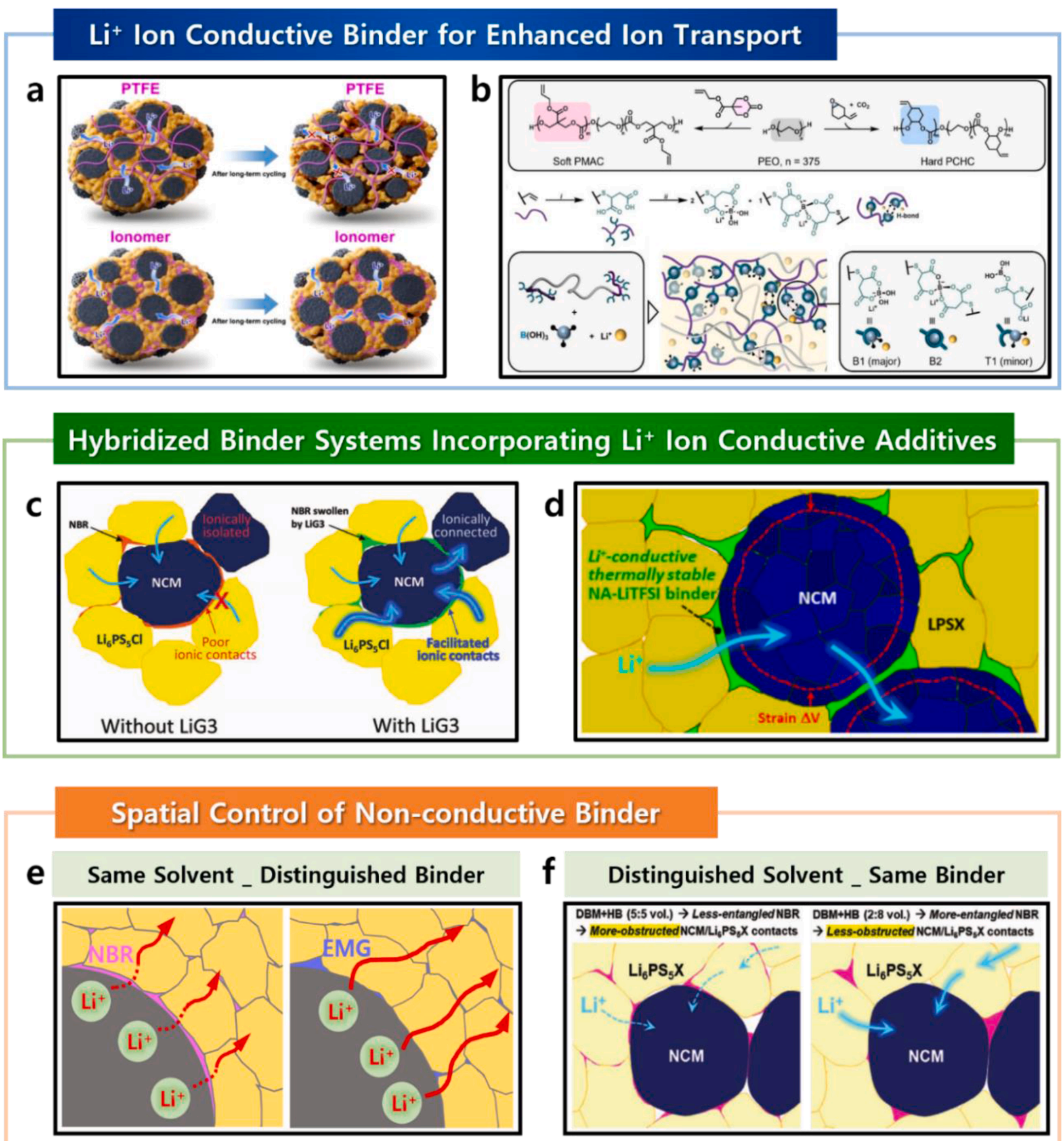

Fig. 3. Representative binder design strategies to enhance Li^+ ion conduction pathways within composite cathodes. Li^+ ion conductive binders (a) using PTFE-based copolymer [47], and (b) incorporating borate-based single-ion conducting polymer [52]. Enhanced interfacial ionic connectivity by (c) incorporating Li^+ ion conductive SIL into the NBR binder [53], and (d) employing a polymer electrolyte [54]. (e) Minimizing blockage of Li^+ ion conduction pathways at the active material-solid electrolyte interface by using EMG binder with spatially localized distribution [55]. (f) Controlling NBR binder dispersion via co-solvent ratio to reduce interfacial obstruction and enhance Li^+ ion transport [57].

promote structural recovery. Such functionality opens a new avenue for designing multifunctional binders that address both mechanical degradation and interfacial instability in high-energy ASSLBs.

2.2. Ion-Conductive architectures for high rate capability

Enhancing the rate capability of sulfide-based ASSLBs requires sophisticated binder designs that go beyond providing mere mechanical integrity. In particular, recent efforts have focused on ensuring continuous and efficient ion conduction pathways within composite cathodes. This strategy marks a shift from conventional approaches that primarily aimed to bind electrode components and improve electrode densification. A major challenge lies in the electrochemical isolation of cathode active materials due to insufficient interfacial connectivity. This issue, which becomes particularly severe at high current rates, leads to increased overpotential and reduced cell efficiency [35]. To overcome this problem, two complementary strategies have emerged: (1) endowing insulating polymer binders with ionic conductivity and (2) spatially controlling binder distribution to avoid blocking Li^+ ion transport pathways. This section highlights recent advancements in these two areas, with a particular emphasis on how polymer binder design governs ionic transport within the composite cathode.

In dry-processed systems, while the absence of organic solvents helps preserve the intrinsic conductivity of sulfide electrolytes, it often results in poor component dispersion and discontinuous ion-conduction networks. To address these limitations, ion-conductive binders specifically tailored for dry processing have been explored. For example, Hong et al. reported an ionomer binder incorporating ion-conductive functional groups as side chains, while maintaining the oxidative stability of perfluorinated polymer (Fig. 3**a**) [47]. Unlike PTFE, which forms physical fibrous networks, the ionomer exhibited dot-like binding that directly interfaces with both active material and solid electrolyte particles. This design enhances mechanical cohesion and facilitates ion transport within the composite electrode, thereby reducing ionic resistance and mitigating heterogeneity commonly observed in PTFE-based systems. Ion conduction in functional polymer binders primarily occurs through polar segments and amorphous domains that provide dynamic coordination sites for Li^+ ion migration [48]. At the same time, the formation of polymer–solid electrolyte interfacial networks facilitates continuous Li^+ ion transport and mitigates local potential gradients, thereby enhancing ionic conductivity across heterogeneous interfaces [49,50]. In addition, the viscoelastic properties of polymer binders effectively buffer interfacial stress and prevent contact loss during cycling, leading to improved interfacial stability and structural integrity. Similar studies using a Nafion binder have also been reported in follow-up research on sulfide-based ASSLBs [51]. In a related study, Thomas et al. developed a fixed-anion-type binder that simultaneously provides mechanical robustness and ionic conductivity in dry-processed electrodes (Fig. 3**b**) [52]. This strategy involved incorporating borate-based ionic sites into a fluorine-free polycarbonate backbone, creating a framework in which fixed anions facilitate selective Li^+ ion conduction. By optimizing the binder's glass transition temperature, the authors achieved a balance between mechanical flexibility and ionic mobility – both critical for maintaining interfacial contact under high mass loading and low-pressure conditions. Such structural tuning effectively addresses bottlenecks in ionic transport while preserving long-term mechanical durability. Promising results have also been reported in wet-processed electrodes. A representative example involves the use of solvate ionic liquid (SIL)-based composite binders engineered for both slurry compatibility and ion conduction (Fig. 3**c**) [53]. In this study, Li(G3) TFSI (G3: triethylene glycol dimethyl ether) salt was incorporated into an NBR matrix, and a low-polarity solvent was used to minimize undesirable reactions with sulfide electrolytes. Magic angle spinning (MAS) NMR measurements confirmed that Li^+ ion conduction occurred through the binder phase, indicating its active role as an ion transport network. In a subsequent study, a dry polymer electrolyte was introduced to address the thermal instability of the SIL-based binder (Fig. 3**d**) [54]. A solid polymer electrolyte based on poly(butylene adipate) incorporating LiTFSI was employed, offering high thermal stability and improved processability. Notably, the binder exhibited robust electrochemical stability and high-rate capability under various extreme conditions, including high mass-loading and temperature fluctuations.

As an alternative design concept, a novel approach focusing on the spatial control of insulating binders within the cathode has been proposed. Due to the inherently low ionic conductivity of polymer binders, their widespread distribution within the composite cathode obstructs ion conduction pathways. Accordingly, this strategy aims to maximize direct contact between active materials and solid electrolytes, thereby ensuring effective ion transport channels. In this context, a design methodology was introduced to localize the binder only to critical regions, thus promoting the efficient formation of continuous ion conduction networks. Hong et al. demonstrated that tailoring binder distribution through variation in functional groups enables the formation of core ion-conduction pathways while maintaining adequate mechanical cohesion (Fig. 3**e**) [55]. Compared to the conventional NBR binder, the poly(ethylene-co-methyl acrylate-co-glycidyl methacrylate) (EMG) binder, which exhibits lower dissociation in the same solvent, showed a more localized distribution without excessively infiltrating the interface between active materials and solid electrolytes. This spatial selectivity facilitated the formation of effective conduction pathways and resulted in improved rate performance. In their report, theoretical calculations based on density functional theory (DFT) supported the experimental findings, confirming that the strong binding affinity of EMG could be predicted in advance, thereby enabling rational binder selection prior to experimental validation [55]. Collectively, these results highlight the importance of controlling the distribution of non-conductive polymer binders to promote ion transport, suppress internal cracking, and maintain interfacial integrity. The compatibility between polymer binder and solvent can be quantitatively assessed using the Flory-Huggins interaction parameter (χ) and the Hansen solubility parameter (δ), both of which describe the thermodynamic affinity between the two species [56]. These parameters enable prediction of the degree of polymer chain dispersion or aggregation under specific solvent environments, providing insight into how molecular interactions govern the uniformity of the binder phase. Such quantitative understanding provides a rational basis for optimizing solvent-polymer combinations to achieve proper binder distribution during slurry casting, thereby enhancing the structural integrity and ionic conduction pathways of the resulting composite electrodes. Another strategy for achieving spatial control involves adjusting the solvent composition during slurry preparation. Kim et al. tailored the ratio of co-solvents, dibromomethane and hexyl butyrate, to modulate the dispersion state of NBR (Fig. 3**f**) [57]. Higher fractions of hexyl butyrate resulted in more compact binder domains, thereby preserving ionic connectivity while maintaining structural cohesion. ToF-SIMS and MAS-NMR analyses confirmed the localized distribution of the binder, and electrochemical evaluations demonstrated enhanced interfacial conductivity and rate capability. These findings underscore the role of polymer binders as spatial regulators that facilitate efficient ion transport. Whether by enhancing their intrinsic ionic conductivity or by controlling their spatial arrangement within the electrode, binders are increasingly recognized as critical enablers of high-rate performance in ASSLBs. Their design, therefore, requires strategic consideration in alignment with both processing methods and cathode architecture.

Finally, Table 2 presents a comparative summary of binder type and content with the achievable areal capacity in sulfide-based ASSLBs, highlighting the strong correlation between them.

2.3. Concluding remark

Polymer binders in composite cathodes, once regarded as passive mechanical integrators, are now recognized as active design elements

Table 2
Binder type and content versus achievable areal capacity in the composite cathodes of sulfide-based ASSLBs.

Active material	Solid electrolyte	Conducting carbon	Binder type	Binder content (wt. %)	Active material loading (mg cm^{-2})	Areal capacity (mAh cm^{-2})	Ref
NCM90	LPSCl	VG-CNF	PTFE	0.1–1.0			[37]
NCA	LPSCl	CNF	PTFE	1.0	15	3	[38]
NCM811	LPSCl	CNF	PTFE	1.0	14	2.8	[39]
NCM821008	LPSCl	Super C	PTFE	1.0			[40]
NCM701515	$LPSCl_{0.5}Br_{0.5}$	Super C65	Polymeric binder	1.5	4.2		[41]
NCM701515	LPSCl	Super P	TBA-*b*-BR binder	2.0	16		[42]
NCM701515	LPSCl	Super P	C10 binder	2.0	2.7		[43]
NCM811	LPSCl	Super C	PTFE	1.0	49	8.7	[45]
NCM701515	$LPSCl_{0.5}Br_{0.5}$	Super P	NBR	2.5			[46]
NCM712	LPSCl	Carbon nanofiber	Ionomer binder	2.0			[47]
NCM701515	LPSCl	Carbon nanofiber	Nafion-Li^{+}	2.0	16.2	2.9	[51]
NCM811	LPSCl	CNF	Lithium borate polymer	5.0		3	[52]
NCM701515	LPSCl	Super C65	NBR + LiG3	6.0	31.5	5.2	[53]

that influence ionic conduction and interfacial stability in sulfide-based ASSLBs. To satisfy the dual requirements of high areal capacity and rate capability, recent studies have introduced fibrillated PTFE, chemically cross-linked systems, and spatially engineered binders that facilitate efficient Li^{+} ion transport. However, challenges remain for large-scale implementation, as factors such as film thickness, pressure gradients, and interfacial heterogeneity affect binder performance. Uneven binder distribution can disrupt conduction pathways and degrade overall cell performance. Future research should adopt a system-level approach, integrating processing–structure–property relationships with quantitative mapping and multiscale modeling. Ultimately, binder design and integration in composite cathodes are critical to realizing next-generation ASSLBs with both high energy and high power densities.

3. Anode

The advancement of sulfide-based ASSLBs toward high energy density relies not only on innovations in cathode design but also on the development of compatible and efficient anode configurations. An

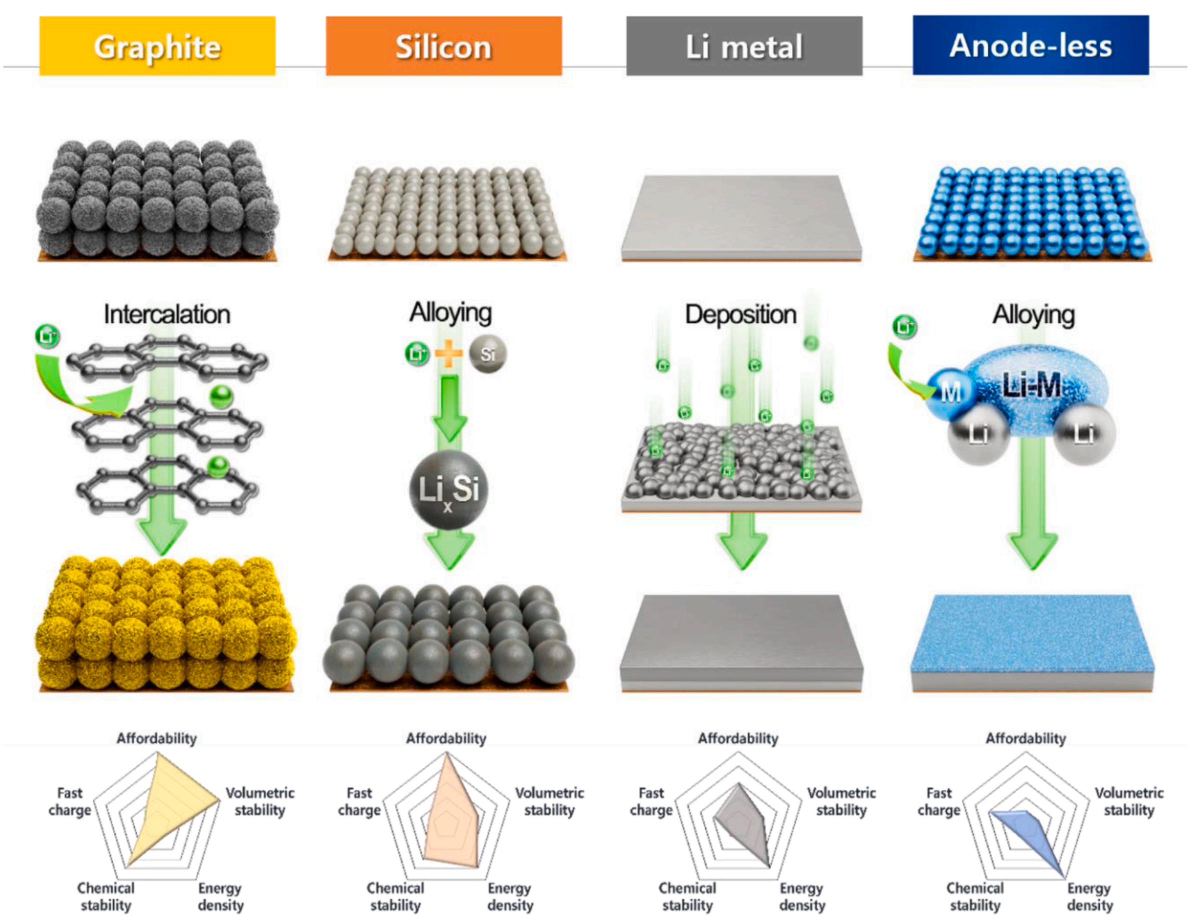

Fig. 4. Schematic illustration of charging mechanisms and comparative properties of different anode systems for ASSLBs.

active anode material with a high specific capacity and a low redox potential is essential for maximizing the energy density of ASSLBs. While extensive research has focused on transition metal oxide-based composite cathodes, such as $LiNi_xCo_yMn_{1-x-y}O_2$, the optimal anode structure for ASSLBs remains less clearly defined [58]. As illustrated in Fig. 4, a wide range of anode materials for ASSLBs has been investigated. In sulfide-based ASSLBs, the anode benefits from the absence of solid electrolyte mixing due to the inherent lithium diffusivity within the anode. This simplification enhances energy density and reduces cost by eliminating the need for expensive solid electrolytes [19,59,60]. However, the broad range of candidate materials and structural configurations introduces significant design complexity and has hindered the establishment of standardized anode frameworks for ASSLBs. In this context, anode systems are categorized into two distinct groups based on the theoretical limit of their lithium storage capacity. Limited-lithium storage (LLS) systems include intercalation and alloy-type anodes, such as graphite and silicon, which possess intrinsic lithium storage capacity [61]. In contrast, unlimited-lithium storage (ULS) systems, such as lithium metal and anode-less configurations, rely on the electrochemical deposition of lithium during cycling and offer theoretically unrestricted capacity [62]. In LLS systems, Li^+ ions migrate across the solid electrolyte–anode interface and are stored via intercalation or alloying with the active material. Therefore, maintaining a stable interfacial environment between the active material and the solid electrolyte, as well as among the active material particles themselves, is essential for facilitating homogeneous lithium-ion flux [63]. However, the inherent volume fluctuations of active materials, particularly silicon, induce mechanical stress and void formation, which disrupt ion and electron transport and accelerate cell degradation [64]. In these systems, polymer binders are expected to provide both strong interfacial adhesion and mechanical compliance, buffering volume expansion while preserving percolation networks for continuous conduction. The mechanical role of binders becomes even more critical in ULS systems, particularly in anode-less configurations, where lithium is electrochemically deposited onto a current collector. These systems undergo extreme volume changes and are highly susceptible to interfacial instability. Lithium deposition occurs via reduction at the surface of the current collector or a lithiophilic alloy (e.g., Li, Ag-C). Although these systems offer superior energy density, they face significant challenges due to parasitic reactions at the lithium–solid electrolyte interface [62,65]. Sulfide-based solid electrolytes are especially vulnerable because of their narrow electrochemical stability window, which leads to chemical decomposition upon contact with freshly deposited lithium metal [66]. To mitigate these interfacial reactions, recent studies have focused on developing protective interlayers that decouple lithium from direct contact with the solid electrolyte while maintaining efficient Li^+ ion transport. In parallel, polymer binders have been engineered to accommodate the substantial volumetric changes during cycling and to maintain chemical compatibility with both lithium metal and sulfide-based electrolytes. As such, hybrid approaches that combine interface-specific binders with protective interlayers have gained attention as an integrated strategy to stabilize lithium deposition morphology and suppress undesired interfacial reactions. Building upon this dual approach, considerable research has focused on developing soft-matter architectures that function not only as mechanical supports but also as active components for interfacial regulation. To accelerate the practical realization of sulfide-based ASSLBs, it is essential to establish system-specific design strategies that optimize both binder properties and protective layer functionalities. This section systematically addresses the design principles for both lithium storage-limited and storage-unlimited anode configurations, with the aim of redefining the role of soft materials in enabling scalable and high-performance ASSLBs.

3.1. Limited-Lithium storage (LLS) anode

Graphite, used in current lithium-ion batteries, stores lithium through intercalation into its layered structure. Despite its relatively low specific capacity (~372 mAh g^{-1}), it has been widely used due to its excellent electrochemical and chemical stability [67]. Graphite undergoes minimal volume expansion during cycling, thereby maintaining good interfacial contact with solid electrolytes, making it a promising candidate for application in sulfide-based ASSLBs [68]. However, its limited lithium storage capacity constrains the achievable energy density, necessitating alternative strategies to enhance lithium storage efficiency. In this context, Kim et al. proposed a diffusion-dependent graphite anode structure that omits solid electrolytes from the electrode formulation [19]. Owing to the mechanical deformability of graphite, the particles maintain intimate contact under pressure, enabling continuous Li^+ ion diffusion. The diffusion-dependent graphite electrode exhibited a comparable areal capacity to that of a composite anode containing 38 wt. % solid electrolyte, while also achieving a higher volumetric capacity. Nevertheless, the interfacial resistance remained relatively high, leading to reduced areal capacities under high current densities. To address this limitation, Shin et al. introduced a Li^+ ion-conducting binder into a diffusion-dependent graphite electrode (Fig. 5**a**) [69]. Li-substituted carboxymethyl cellulose (Li-CMC) was synthesized via a two-step ion-exchange process. First, Na-CMC was obtained by substituting H^+ in virgin CMC with Na^+ under acidic conditions. Then, Li-CMC was prepared by reacting Na-CMC with $LiOH{\cdot}H_2O$ solution. The Li-CMC binder exhibited strong adhesive properties even at low binder content due to its CMC backbone, while the presence of substituted Li^+ ions facilitated interfacial Li^+ ion transport. These improvements enabled the electrode to reach the theoretical capacity of graphite under high mass loading conditions. These findings reveal that efficient Li^+ ion transport at the interfaces of graphite-based anodes is critical for achieving high electrochemical performance. Despite these advances, graphite-based anodes remain fundamentally limited by their low capacity. As a result, considerable research efforts have focused on incorporating silicon as an anode material in ASSLBs [61]. Silicon exhibits a high theoretical specific capacity of about 4200 mAh g^{-1}, making it a highly attractive anode candidate for high-energy ASSLBs. Tan et al. fabricated μ-Si-based anodes for ASSLBs [70]. During the initial charging process, μ-Si formed a Li–Si alloy phase, providing continuous pathways for both Li^+ ion and electron transport within the electrode and enabling uniform lithiation. The absence of conductive carbon and solid electrolytes in the anode minimized the formation of by-products such as Li_2S, which are typically generated by the reductive decomposition of sulfide electrolytes at the solid–solid interface. As a result, the μ-Si anode exhibited high coulombic efficiency and stable cycling behavior, highlighting its potential to enhance the energy density of ASSLBs. These findings demonstrate the feasibility of significantly improving the energy density of ASSLBs by employing a pure Si-based anode. Despite these advantages, the practical application of Si remains limited due to its substantial volume expansion during cycling, which leads to cracking and deterioration of interfacial contact with solid electrolytes [71,72]. Although nanostructured Si (e.g., nanowires or nanoparticles) has been proposed to alleviate stress accumulation and accommodate volume changes, interfacial degradation remains a key challenge [73,74]. To address this issue, recent research has focused on using materials capable of effectively accommodating the volume changes of Si. Pre-lithiated Si with low modulus provides mechanical buffering capability and facilitates both ionic and electronic transport within the anode [74,75]. Yan et al. developed Si-based anodes composed of pre-lithiated silicon and hard carbon [76]. The pre-lithiated Si mitigated interfacial degradation caused by the pronounced volume expansion of silicon during cycling, while simultaneously forming a percolating network that facilitated both Li^+ ion and electron transport. Complementarily, hard carbon acted not only as a mechanical buffer but also as a secondary lithium reservoir, effectively

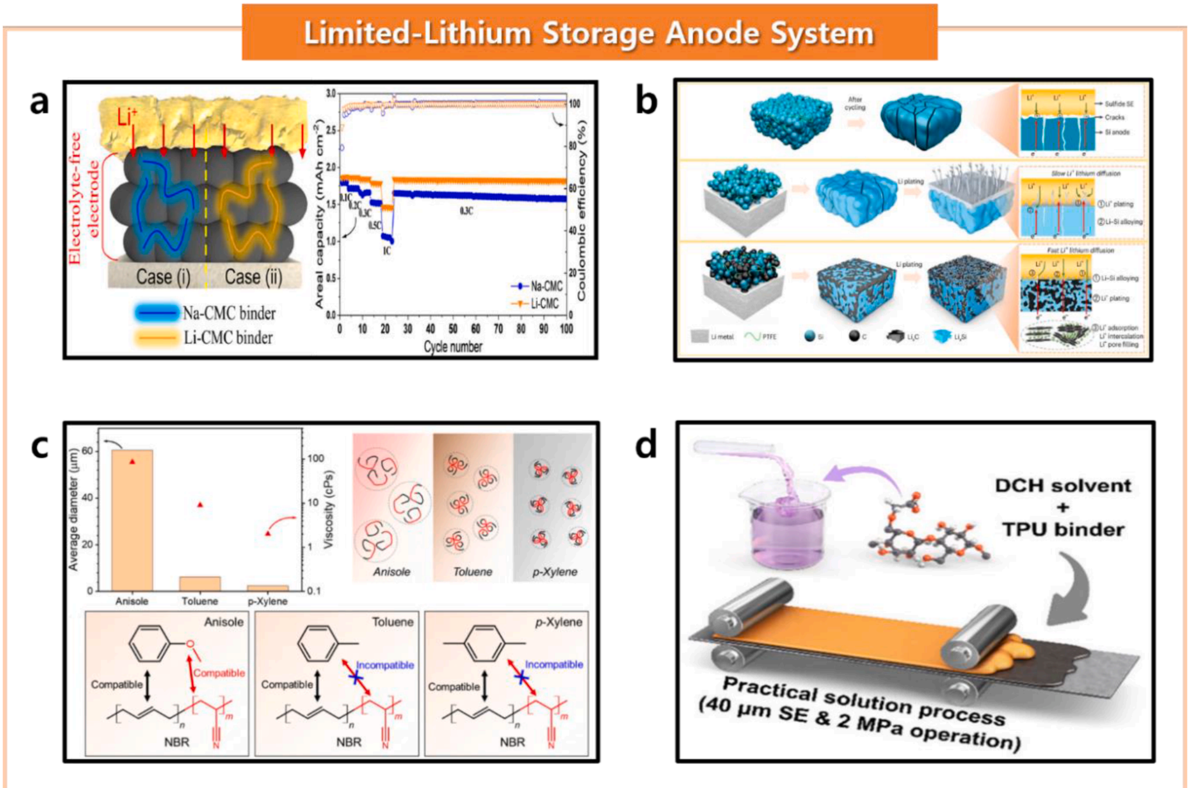

Fig. 5. Representative research strategies for polymer binders in graphite and silicon-based LLS anode systems. (a) Graphite electrodes employing a non-conducting binder (Na-CMC) or a Li^+ ion conducting functional binder (Li-CMC), along with their electrochemical performance [69]. (b) Cycling mechanisms in ASSLBs for Si, pre-lithiated Si (LiSi) anodes, and LiSi-hard carbon composite anodes [76]. (c) Polymer size and viscosity of binder solutions, and schematic illustrations of polymer domains and solvent compatibility in NBR copolymer units [80]. (d) Double-cast process using DCH solvent and TPU binder [82].

suppressing dendritic growth and stabilizing the electrode structure. This dual-component architecture established a three-dimensional conduction network within the anode, enabling homogeneous electrochemical activity and reducing the risk of soft short circuits (Fig. 5**b**). As a result, the anode exhibited excellent cycling stability in sulfide-based ASSLBs, demonstrating that Si–carbon hybridization can simultaneously address both interfacial instability and structural degradation in high-capacity anodes. This approach has sustained interest in Si–graphite (Si–Gr) composites, which offer a promising balance between energy density and structural stability. In these systems, lithium first alloys with silicon, followed by intercalation into graphite during charging [77]. This sequential lithiation process effectively mitigates the risk of internal short-circuits caused by lithium metal plating on graphite surfaces [78]. Moreover, the inherent electronic conductivity of graphite compensates for that of silicon, while also reducing overall volume expansion compared to pure Si-based electrodes. These advantages are further enhanced under stack pressure, which is commonly applied in ASSLBs configurations [79]. Consequently, the Si–Gr composite has emerged as a promising candidate for high-energy sulfide-based ASSLBs. However, interfacial instability arising from the inherent volume changes of silicon remains a persistent challenge. To address this issue, Choi et al. proposed a solvent polarity–driven binder design strategy aimed at enhancing interfacial adhesion between the active material and binder [80]. They improved the solubility of the NBR binder by using anisole, which has a higher polarity than the conventionally used toluene. The increased solvent–binder affinity promoted the formation of larger NBR domains with enhanced activation of nitrile functionalities (Fig. 5**c**), thereby strengthening both cohesion and interfacial adhesion within the electrode. As a result, the anode fabricated using NBR dissolved in anisole exhibited superior mechanical integrity, attributed to the improved activation of nitrile groups in the binder. It demonstrated higher capacity retention and greater coulombic efficiency than its toluene-processed counterpart, even under reduced stack pressure. As discussed in the composite cathode section, a large amount of polymer binder generally hinders Li^+ ion transport pathways. Nevertheless, this study suggests that in electrodes incorporating high-volume-change active materials such as Si, interfacial adhesion should be prioritized over ionic conductivity to suppress void formation and maintain continuous Li^+ ion transport within the electrode. In addition, interfacial contact becomes even more critical under low-pressure conditions, which are essential for the practical implementation of ASSLBs. Accordingly, the use of highly polar polymer binders is beneficial for enhancing interfacial contact. However, highly polar solvents are limited in sulfide-based ASSLBs due to their poor chemical compatibility with sulfide-based solid electrolytes [81]. To overcome this challenge, Oh et al. introduced a new solvent–binder system optimized for Si–Gr composite anodes (Fig. 5**d**) [82]. They employed 1,6-dichlorohexane (DCH) as a solvent with unique conformational behavior: its gauche conformer exhibits a high dipole moment that enables the dissolution of highly polar polymers, while its anti-conformer maintains chemical compatibility with sulfide-based electrolytes due to its relatively low polarity. This dual-character solvent allowed the application of thermoplastic polyurethane (TPU) as a binder, which provides strong ion–dipole interactions through urethane functional groups. TPU was effectively dissolved in DCH and incorporated into the composite anode despite its high polarity. The resulting electrode exhibited minimal thickness variation during cycling, attributed to enhanced interfacial cohesion. It maintained stable operation of ASSLBs at room temperature and under significantly reduced stack pressure. These studies highlight that polymer binder design in LLS-type anodes should not only aim to provide mechanical stabilization through interparticle adhesion but also contribute to the formation of continuous conduction pathways. This role becomes particularly critical under the low-pressure conditions required for the practical operation of ASSLBs, underscoring the emerging paradigm of polymer binders as multifunctional, ion-conductive design elements.

3.2. Unlimited-Lithium storage (ULS) anode

Lithium metal is widely regarded as an ideal anode material for ASSLBs due to its high specific capacity and low redox potential [83]. However, direct contact between lithium metal and sulfide-based solid electrolytes readily triggers unfavorable side reactions, leading to the formation of decomposition products such as Li_2S and Li_3P [66,84]. These interfacial reactions increase interfacial resistance and induce localized current inhomogeneities, thereby accelerating dendritic lithium growth and compromising cycling stability [85]. To address these challenges, recent studies have explored the protective interlayers capable of decoupling lithium metal from the solid electrolyte while permitting efficient Li^+ ion transport. For example, Ji et al. proposed a dendrite formation mechanism and outlined three essential design criteria for effective protective layers: (1) thermodynamic stability against lithium, (2) high ionic conductivity coupled with low electronic conductivity, and (3) high interfacial energy with lithium to suppress uncontrolled nucleation (Fig. 6**a**) [86]. Interlayers based on LiF and Li_3N, which meet these criteria, were fabricated and shown to suppress electrolyte decomposition and enable more stable cycling. In pursuit of higher energy density, recent strategies have focused on creating compact, nanometer-scale protective layers that act as artificial solid electrolyte interphase (SEI). These SEI layers, composed of compounds

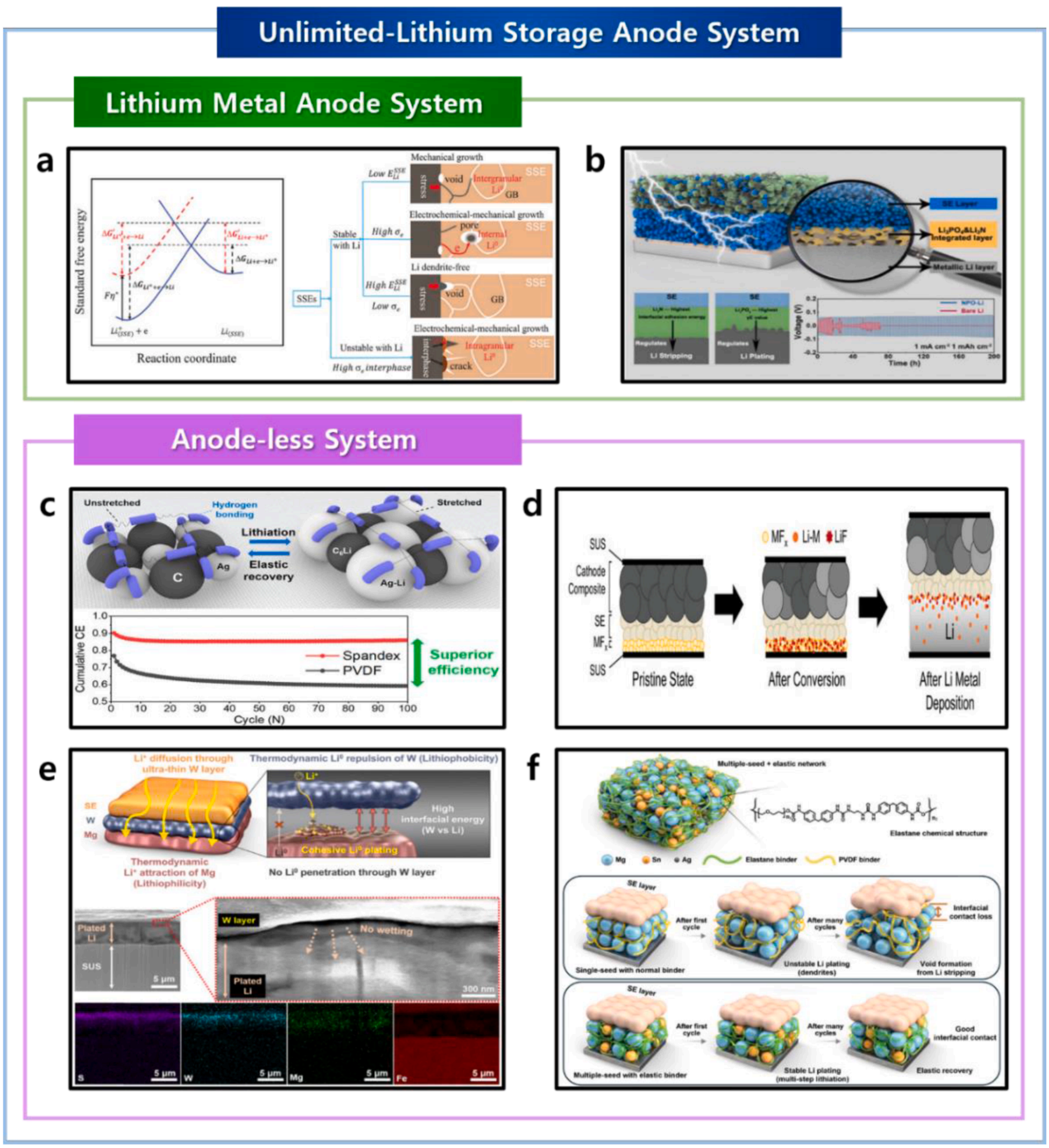

Fig. 6. Research strategies for polymer binders and protective layers in lithium metal and anodeless-based ULS anode systems. (a) Li dendrite formation mechanism in solid electrolytes [86]. (b) Schematic configuration of ASSLBs using Li_3PO_4 and Li_3N-coated Li metal, Li plating/stripping behavior, and corresponding electrochemical performance [89]. (c) Elastic recovery of the spandex during lithiation/delithiation, and electrochemical performance of Ag-C layers with PVdF and spandex binders [96]. (d) LiF formation and conversion mechanism during Li plating on MF_x-based electrode [97]. (e) Mechanism for suppressing Li dendrite growth using W interlayer on Mg-based anodeless layer, and cross-sectional SEM and EDS images after Li plating [100]. (f) Comparison of interfacial properties during cycling between an anodeless layer using multi-seed structures with an elastane binder, and one employing a single-seed structure with a PVdF binder [102].

such as LiF, Li_3N, Li_2O, and Li_3PO_4, have demonstrated effectiveness in mitigating interfacial reactions and suppressing dendrite growth [87–90]. Su et al. successfully fabricated a hybrid protective layer composed of Li_3PO_4 and Li_3N by sequentially spraying H_3PO_4/THF and $LiNO_3$/THF solutions onto lithium metal, followed by solvent evaporation [89]. The lithium metal with the protective layer exhibited high ionic conductivity and interfacial stability with sulfide-based solid electrolytes, owing to the presence of Li_3PO_4 and Li_3N, which possess high interfacial energy toward lithium metal (Fig. 6**b**). Similarly, Sim et al. demonstrated that a dip-coating method using nitromethane and dimethoxyethane formed a compact SEI that effectively suppressed dendrite growth and stabilized the lithium interface [90]. These solution-based surface treatments are particularly attractive due to their simplicity and scalability for large-area lithium electrodes. Despite these advances, the practical application of lithium metal still faces technical challenges. During cycling, lithium tends to propagate into the pores of solid electrolytes under elevated stack pressure, particularly when thin electrolyte sheets are employed [91,92]. To address this issue, the development of mechanically robust protective layers and the fabrication of dense, pore-free solid electrolyte sheets are essential to prevent lithium penetration.

Anode-less systems, in which lithium is electrochemically plated onto a current collector or metal seed, have emerged as a promising strategy to maximize energy density [93]. In these systems, lithium is initially stored as Li–M alloys, followed by homogeneous lithium deposition [94]. Among notable examples, Lee et al. developed Ag–C-based anode-less architectures that employed a carbon black interlayer to prevent direct contact between the plated lithium and the solid electrolyte [95]. During charging, lithium first alloys with silver before metallic deposition occurs, and the resulting volume-expanded alloy is extruded toward the current collector to relieve internal stress [94]. This charging mechanism effectively prevents direct contact between the deposited lithium and the solid electrolyte, thereby suppressing undesirable side reactions. However, internal expansion within the Ag–C layer may lead to a loss of interfacial contact. To address this issue, Oh et al. developed a spandex-based binder composed of flexible polyethylene glycol (PEG) segments and urethane/urea functional groups capable of forming hydrogen bonds with Ag particles (Fig. 6**c**) [96]. The spandex consists of soft segments derived from PEG and hard segments containing urethane and urea groups, which facilitate hydrogen bonding within the Ag–C composite. These hydrogen bonds promote the uniform dispersion of Ag particles and the formation of a dense, low-porosity Ag–C layer. As a result, the Ag–C composite exhibited improved particle dispersion, reduced porosity, and excellent mechanical integrity. The electrodes incorporating the spandex binder demonstrated lower overpotential, enhanced coulombic efficiency, and significantly reduced void formation after cycling, compared to those using a conventional PVdF binder. These findings underscore that even in ULS configurations, robust polymer binders that provide cohesive strength and interfacial integrity are critical for stable battery operation. Beyond their mechanical function, chemically engineered interlayers have also been investigated for their ability to regulate interfacial chemistry. For example, Lee et al. demonstrated that silver fluoride (AgF) can be converted in situ into a uniform LiF layer between the deposited lithium and the solid electrolyte (Fig. 6**d**) [97]. This LiF interlayer, facilitated by the low nucleation overpotential and high lithiophilicity of Ag, enabled uniform lithium plating and suppressed side reactions. However, the excessive lithiophilicity of Ag can lead to inhomogeneous alloying and dendritic growth. To address this issue, alternative metal seeds such as Mg have been explored [98]. Due to its low lithium diffusivity, Mg supports lithium accumulation within the seed layer and promotes stable deposition by generating lithium concentration gradients. In addition, MgF_2-based anode-less layers have been proposed to form protective LiF interlayers upon contact with lithium [99]. These results indicate that tailored interlayers can effectively suppress detrimental interfacial reactions, regardless of the seed material used. In a related study, Oh et al. introduced a tungsten interlayer with high interfacial energy toward lithium metal on an Mg-based anode-less layer (Fig. 6**e**) [100]. The 30 nm-thick tungsten layer enabled sufficient Li^+ ion diffusion while effectively isolating the deposited lithium from the solid electrolyte. This interfacial architecture inhibited chemical decomposition and suppressed dendrite formation, offering a viable pathway for high-rate and stable ASSLBs operation. To accommodate volume changes during cycling, a $Ti_3C_2T_x$ MXene buffer layer was introduced beneath the Mg-based layer [101]. MXene exhibited excellent shape recoverability under external pressure due to its high elasticity. As a result, MXene helped maintain smooth contact between the solid electrolyte and the anode-less layer, enabling stable ASSLBs operation under low external pressure conditions. This approach mirrors LLS strategies and underscores the importance of volume-adaptive interfacial materials for ASSLBs operating under low pressure. Recently, various metal seeds have been actively explored for anode-less systems to improve the cycling stability of ASSLBs. In this system, the establishment of optimized design criteria for metal seeds has become essential. Recent studies have proposed the use of multiple metal seeds with distinct lithiation potentials, rather than relying on a single metal seed, to facilitate more uniform lithium deposition [102]. This multi-seed strategy enabled a broader range of lithiation pathways and promoted uniform lithium nucleation across different voltage ranges. As depicted in Fig. 6**f**, polymer binders with superior adhesive properties are also being investigated to enhance interparticle contact within the metal seed layer.

In summary, binder design for ULS systems should extend beyond conventional mechanical functions to include interfacial regulation and dispersion control within complex architectures. When integrated with protective interlayers and seed materials, these multifunctional binders can effectively address critical challenges, such as dendrite suppression, interfacial stabilization, and volume accommodation, paving the way toward safe, high-energy sulfide-based ASSLBs. A comprehensive summary of reported binder types, binder contents, and corresponding areal capacities of anodes in sulfide-based ASSLBs is provided in Table 3, highlighting the diverse design strategies and their resulting electrochemical performance.

3.3. Concluding remark

To realize practical sulfide-based ASSLBs, various anode systems have been developed with a focus on increasing energy density. In LLS systems, binder design has remained relatively simple, primarily serving as mechanical buffers to accommodate volume changes. In contrast, cathode binders have evolved to enhance both interfacial contact and Li^+ ion transport. This distinction underscores the importance of binders in preventing stress-induced interfacial degradation within anodes. ULS and anode-less systems require multifunctional binders that suppress parasitic reactions and ensure uniform lithium deposition [108]. Anode-less configurations, free from pre-existing lithium or composite anodes, offer the highest energy density. As shown in Fig. 7, their compatibility with low-pressure operation and lack of sulfide electrolyte in the anode layer reduce binder-related challenges. Ultimately, advancing high-performance anode systems requires an integrated strategy combining materials design, processing, and interfacial engineering. Accordingly, the polymer binders for anode must be redefined as active elements that control ion transport, structural integrity, and cycle life, essential for commercializing next-generation ASSLBs.

4. Solid electrolyte sheets

Previous studies on electrodes incorporating polymer binders have demonstrated notable improvements in cycling stability and rate capability, primarily attributed to the formation of optimized ion conduction pathways and enhanced mechanical stability. These findings have driven a paradigm shift in the design of solid electrolyte sheets, which

Table 3
Summary of binder types, binder content, and corresponding areal capacities of anodes in sulfide-based ASSLBs.

Active material	Solid electrolyte	Conducting carbon	Binder type	Binder content (wt. %)	Active material (mg cm^{-2})	Areal capacity (mAh cm^{-2})	Ref
Graphite	-	-	Li-CMC + SBR	3.0	5.1	1.8	[69]
Si + HC	-	-	PTFE	5.0	2.1	0.7	[76]
Gr + Si	LPSCl	-	NBR	4.0	2.2		[80]
Gr + Si	LPSCl	-	TPU	2.5			[82]
Ag + Carbon black	-	-	PVdF	7.0			[95]
Ag	-	Carbon	Spandex	2.0		0.86	[96]
AgF	-	-	PVdF	2.5	0.24	0.98	[97]
Mg	-	-	PVdF	10	0.36–0.45	1.8	[98]
MgF_2	-	Carbon	PVdF	19		1.4	[99]
Mg + Ag + Sn	-		Elastane	10	0.45	2.7	[102]
Graphite	-	Super P	PVdF	10			[103]
Graphite	$LPSCl_{0.5}Br_{0.5}$	-	NBR	2.5			[104,105]
Si	-	-	PVdF	0.5	1.6		[106]
Si	-	-	Ag@PAP	20	0.4–0.6	0.8–1.2	[107]

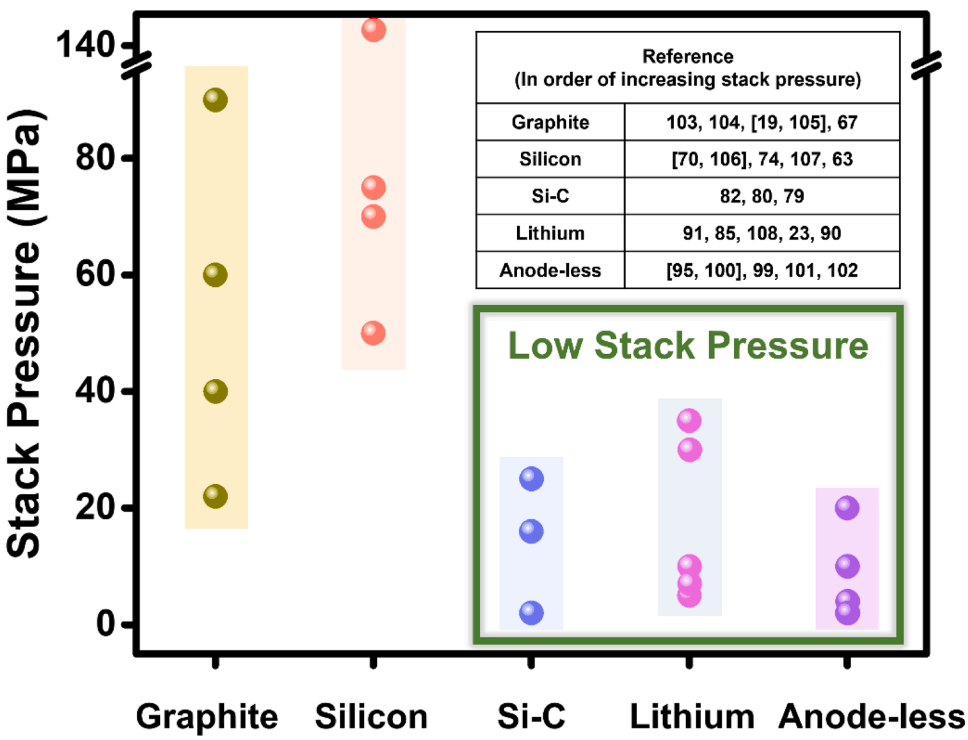

Fig. 7. Comparison of stack pressure for various anode configurations in ASSLBs.

serve as critical components between the two electrodes in ASSLBs. While traditional solid electrolyte sheet fabrication has prioritized mechanical robustness through the use of binder-based scaffolding, such approaches often result in significant compromises in ionic conductivity. In this section, we deal with recent strategies aimed at enhancing ion transport in solid electrolyte sheets while preserving their mechanical integrity in thin-sheet form, categorized into three main approaches.

4.1. Dry-processed solid electrolyte sheets

One widely adopted method for preparing free-standing solid electrolyte sheets is the dry process, in which polymer fibrillation is induced by applying shear force to PTFE binder. A key advantage of the PTFE-based dry process is the elimination of solvents during fabrication, thereby avoiding the degradation of solid electrolytes caused by solvent exposure. Thanks to these benefits, numerous studies have reported that this method enables the fabrication of thin sheets and offers excellent scalability for large-area applications. For instance, Zhang et al. demonstrated the fabrication of an ultrathin (30 μm) sulfide-based solid electrolyte sheet with exceptionally high ionic conductivity (8.4 mS cm^{-1}) using a dry process involving PTFE binder (Fig. 8**a**) [109]. Moreover, they demonstrated that electrolyte sheets with dimensions of approximately 5 × 7 cm^2 can be continuously and scalably fabricated via a hot calendaring process, highlighting their potential for industrially feasible large-scale production. Building on a similar technique, Lee et al. emphasized the importance of controlling PTFE fibrillation to achieve optimal electrochemical stability, addressing challenges such as ion blockage and current leakage that could compromise cycling performance. Their study highlighted the significant influence of processing parameters on the performance of dry-processed solid electrolyte sheets, paving the way for enhanced cycling stability (Fig. 8**b**) [110]. However, PTFE-based sheet fabrication presents two major drawbacks that hinder its practical application at the cell level. First, PTFE exhibits poor reductive stability at low potentials (< 1.0 V vs. Li/Li$^+$), which can lead

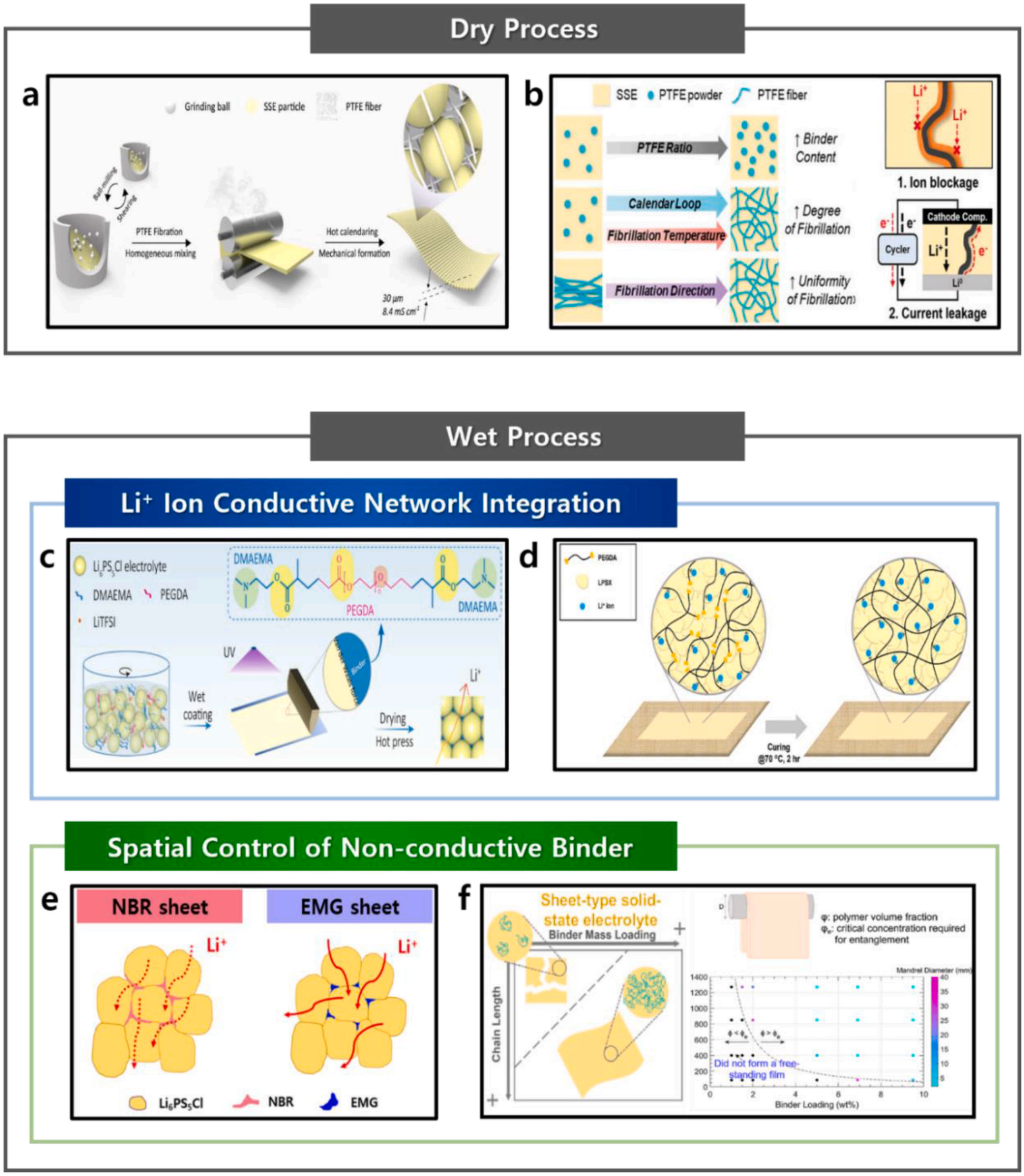

Fig. 8. Dry-processed solid electrolyte sheets: (a) fabrication of a solid electrolyte sheet using PTFE binder [109], and (b) limitations of PTFE-based solid electrolyte sheets [110]. Cross-linked solid electrolyte sheets: (c) formation of a three-dimensional polymer network via in-situ cross-linking [113], and (d) introduction of lithium salt into the polymer network to provide additional Li^+ ion conduction pathways [114]. Spatial regulation of non-conductive polymer binders in sulfide-based solid electrolyte sheets: (e) optimization of Li^+ ion transport pathways through controlled local distribution of EMG binder [115], and (f) enhancement of mechanical robustness via polymer chain entanglement [116].

to increased cell resistance and deteriorated electrochemical performance [111,112]. Second, the dry process suffers from limited film homogeneity due to the uneven distribution of fibrillated polymer binders [40]. As a result, it is common practice to punch and evaluate multiple regions of the PTFE-based sheet to assess film quality, underscoring the difficulty in achieving uniformity across large-area films ($>$ 50 cm^2), a critical requirement for the practical development of ASSLBs.

4.2. Wet-processed solid electrolyte sheets

An alternative approach for fabricating solid electrolyte sheets is the wet casting method, which involves dissolving polymer binders and mixing them with solid electrolytes prior to film formation. Although this method typically yields lower ionic conductivity, it offers improved film homogeneity and greater simplicity in processing. Accordingly, this section introduces advanced strategies aimed at overcoming the conductivity limitations of wet-processed solid electrolyte sheets. One such strategy involves enhancing ionic conductivity through chemical bonding of organic components to maximize interfacial adhesion. Xiaolei et al. developed a composite solid electrolyte sheet using a polymer matrix composed of poly(ethylene glycol) diacrylate (PEGDA), dimethyl aminoethyl methacrylate (DMAEMA), and LiTFSI via in-situ polymerization and slurry casting (Fig. 8**c**) [113]. This chemically bonded structure enabled uniform dispersion of solid electrolytes within the polymer matrix, resulting in a continuous ion-conductive network and improved mechanical cohesion. Notably, this design ensured interfacial stability even under solvent exposure in wet processing. A similar approach based on cross-linked bonding has been reported, in which the chemical cross-links serve as a conductive network in addition to the inorganic electrolyte, thereby enhancing overall ionic conductivity. Specifically, this strategy involves the chemical cross-linking of an ion-conductive polymer to construct an additional ion-conducting network alongside the inorganic solid electrolyte. Lee et al. introduced a PEGDA-based polymeric network to overcome the limitations of conventional non-conductive binder systems. By mixing PEGDA with LiTFSI followed by thermal treatment, a three-dimensional ion-conductive network was formed, satisfying both mechanical adhesion and ion transport requirements (Fig. 8**d**) [114]. This polymer network exhibited comparable thickness and flexibility to PTFE-based solid electrolyte sheets, offering advantages in scalability and thin-film fabrication, and thus demonstrating compatibility with commercial manufacturing processes. It effectively addressed the uniformity issues observed in dry-processed PTFE sheets and the reduced ionic conductivity typically associated with conventional wet-cast films. Furthermore, the development of such an organic–inorganic hybrid conductive system established a successful precedent, demonstrating the feasibility of designing hybrid solid electrolytes that bridge organic and inorganic networks, an insight that may prove pivotal in the future design of solid electrolyte sheets. In addition to constructing ion-conductive networks, recent efforts have focused on the control of non-conductive binder distribution within solid electrolyte sheets to minimize resistance pathways. Hong et al. reported a strategy using poly(ethylene-co-methyl acrylate-co-glycidyl methacrylate) (EMG), which tends to aggregate and form localized regions with high binder concentration, thereby reducing the overall volume of ionically insulating domains (Fig. 8**e**) [115]. The acrylate of EMG enhanced interfacial adhesion, enabling stable Li^+ ion transport and mechanical robustness through conventional slurry casting. Anna et al. aimed to simultaneously enhance structural integrity and ionic conductivity by leveraging the physical properties of polymer binders, specifically focusing on polymer chain entanglement (Fig. 8**f**) [116]. By systematically varying the molecular weight and concentration of a poly (isobutylene) binder, they evaluated its effects on both mechanical strength and ion conduction within the solid electrolyte sheet. Their findings revealed that increasing the molecular weight promoted greater chain entanglement, resulting in improved mechanical stability. However, excessively high molecular weight led to increased grain boundary resistance and reduced critical current density, ultimately compromising ionic conductivity. These results underscore the critical importance of balancing the mechanical properties of polymer binders with the preservation of efficient ion conduction pathways in solid electrolyte sheets.

4.3. Solid electrolyte sheets via scaffold-assisted architectures

A scaffold-assisted fabrication method for ultrathin solid electrolytes has been reported, in which Kang et al. proposed preparing a polymer framework followed by the infiltration of a solid electrolyte slurry (Fig. 9**a**) [117]. The electrolyte was uniformly embedded within the scaffold, resulting in an ultrathin sheet with high ionic conductivity and mechanical durability. A follow-up study optimized the internal void structure of the scaffold by employing a laser-processed high-porosity film to enhance slurry infiltration and structural support (Fig. 9**b**) [118]. By using a high-porosity film as the scaffold, this process achieved both efficient slurry infiltration and reliable retention of the solid electrolyte. Another approach employed an electrospun polyimide membrane as a thermally stable scaffold for solid electrolyte infiltration (Fig. 9**c**) [119]. This strategy enabled the pre-structuring of a mechanically robust scaffold with a controllable pore architecture tailored for efficient ion conduction. As a result, a 40 μm-thick solid electrolyte sheet combining structural stability and flexibility was fabricated without compromising ionic conductivity. In a separate study, a high-strength polymer fiber material was used as the reinforcing agent, followed by hot pressing to densify the composite structure (Fig. 9**d**) [18]. This approach enhanced mechanical durability and reduced interfacial voids, thereby improving

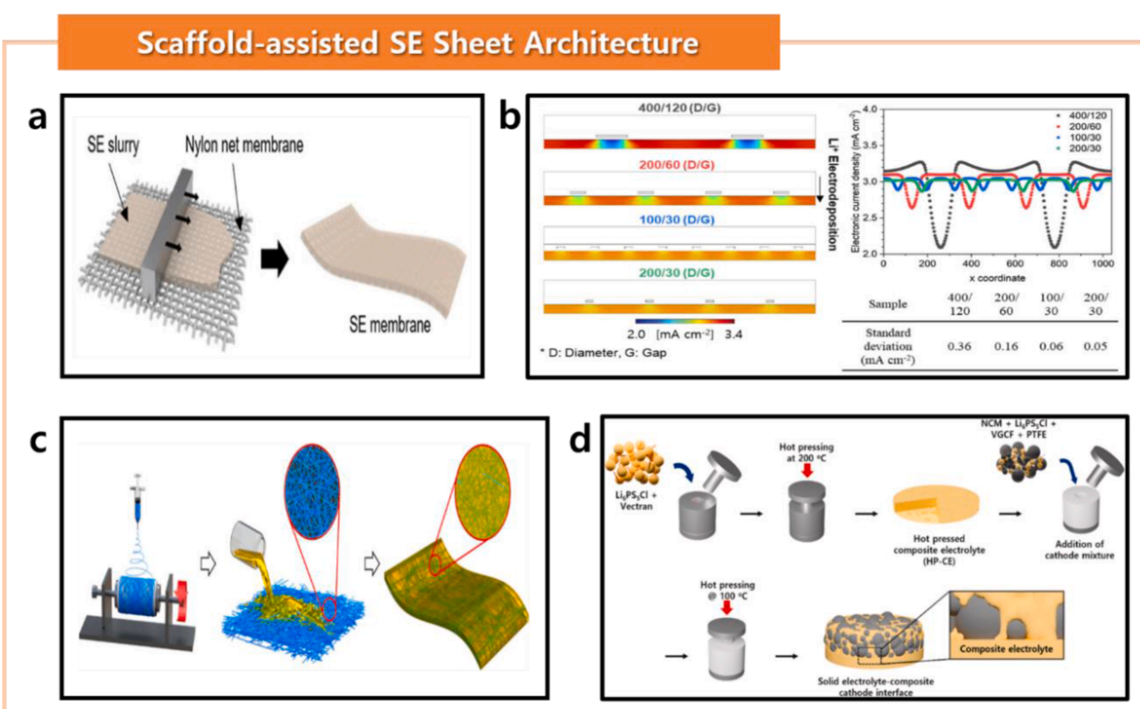

Fig. 9. Scaffold-assisted fabrication of solid electrolyte sheets. (a) Formation of solid electrolyte sheets using nylon-based scaffold [117]. (b) Engineering of scaffold architecture via laser-processed high-porosity films [118]. (c) Fabrication of solid electrolyte sheets by infiltrating solid electrolytes into an electrospun PI membrane with high thermal and mechanical stability [119]. (d) Implementation of a high-strength polymer fiber followed by hot pressing, enabling densification of the composite [18].

ion transport across the solid electrolyte sheet.

4.4. Concluding remark

A representative design strategy for polymer binders aims to ensure both ionic conductivity and structural integrity in thin solid electrolyte sheets. Recent research emphasizes chemical functionalization, spatial distribution, and physical property control to form efficient ion-conductive networks [120]. These advances highlight the need to redefine polymer binders as active ion-conductive components rather than passive mechanical supports. The ionic conductivities and thicknesses of solid electrolyte sheets fabricated by different processes are summarized in Table 4. As shown in the table, the thickness of the electrolyte sheets is generally greater than 30 μm. Therefore, further reduction below this level is essential to enhance the energy density of ASSLBs for practical implementation [121]. As production scales up, maintaining uniform ionic conductivity and mechanical integrity over large areas becomes increasingly important. Future efforts should focus on understanding binder–electrolyte interactions, assessing processing effects on ion transport, and developing hybrid binders with both conductivity and stability, paving the way for the industrial realization of high-performance ASSLBs.

5. Outlook and future directions for binders in ASSLBs

5.1. Large-Scale production

From a practical standpoint, it is essential to design polymer binders that enable uniform dispersion of components during the scalable fabrication of composite electrodes and solid electrolyte sheets. In the dry process, both the electrode and solid electrolyte sheets are typically fabricated through the following sequence. First, the powder components are homogeneously mixed to ensure uniform dispersion of the active materials, conductive additives, and binders. Next, the mixed powders are compressed into freestanding films using a roll-to-roll process. Finally, in the case of electrode fabrication, the film is laminated onto the current collector. A major challenge in large-scale roll-to-roll fabrication lies in maintaining uniform pressure and consistent interfacial contact across the entire surface. Uneven pressure distribution can compromise the mechanical integrity of the electrode and lead to variations in density and interfacial resistance. From this viewpoint, the polymer binder must distribute the applied pressure uniformly throughout the film during the roll-to-roll process, thereby ensuring intimate particle contact and mechanical stability in large-area electrodes. In the wet process, although solvents facilitate the dispersion of polymer binders within the slurry, precise control over solvent-binder interactions is required to achieve uniform dispersion. Emley et al. reported that excessive solvent increases the distance between solvent molecules and polymer chains, weakening binder-particle interactions, whereas insufficient solvent causes binder aggregation due to excessive molecular proximity [122]. Therefore, tailoring the interactions between the polymer binder and solvent is crucial for achieving homogeneous dispersion and a mechanically stable microstructure in composite electrodes and solid electrolyte sheets. In addition, mitigating polymer binder migration during solvent evaporation is essential. Slurries are often dried rapidly at high temperatures to improve process efficiency [123]; however, such conditions can induce binder migration, resulting in compositional inhomogeneity that deteriorates both the mechanical integrity and electrochemical uniformity of the electrode. Hence, developing polymer binders that minimize migration during rapid drying is critical for maintaining electrode uniformity and long-term performance.

5.2. Low stack pressure operation

The fabrication and evaluation of composite electrodes and solid electrolyte sheets incorporating polymer binders for ASSLBs have been actively investigated, as discussed in the previous sections. Most of these studies utilized pellet-type torque cells with small-sized film, operated under stack pressures exceeding 10 MPa, conditions that are far from practical cell configurations. To facilitate the transition of ASSLBs from laboratory validation to commercial implementation, large-area films must operate reliably in pouch or prismatic cell formats [22]. Accordingly, the development of binder systems capable of maintaining reliable performance under low stack pressure and large-area conditions is of critical importance (Fig. 10**a**). The most significant distinction between torque cells and scalable pouch cell formats lies in the limitation of applicable stack pressure. In lab-scale torque cells, stack pressures typically range from 10 to 70 MPa, which can effectively compensate for mechanical gaps caused by electrode volume changes during cycling. In contrast, pouch and prismatic cells generally operate under significantly lower stack pressures (< 4 MPa), presenting markedly different processing conditions compared to the lab-scale environment involving tens of MPa [55,124]. Therefore, ASSLBs must ensure sufficient interfacial contact between the electrodes and solid electrolyte sheets even under low stack pressure conditions. Achieving this requires adherence to several technical criteria. First, uniform composition and density are essential to prevent interfacial delamination and surface mismatch.

Table 4
Summary of solid electrolyte sheet properties prepared by different fabrication methods.

Fabrication method	Solvent	Electrolyte sheets	Thickness (μm)	Ionic conductivity (mS cm^{-1})	Ref.
Dry-process	-	$Li_{5.4}PS_{4.4}Cl_{1.6}$ + PTFE	30	8.4 @ 25 °C	[109]
		Li_6PS_5Cl + PTFE		1.28 - 1.71 @ 25 °C	[110]
		Li_6PS_5Cl + PTFE	25	2.3 @ 25 °C	[112]
Wet-process	Acetonitrile	Li_6PS_5Cl + DMAEMA + PEGDA + LiTFSI	40	1.23 @ RT	[113]
	N-butyl butyrate	$Li_6PS_5Cl_{0.5}Br_{0.5}$ + PEGDA + LiTFSI	75	0.83 @ 25 °C	[114]
	Dichlorobenzene + *n*-butyl butyrate	Li_6PS_5Cl + EMG	110	1.88 @ 60 °C	[115]
	Toluene	PIB	81 - 114	0.08 - 0.5 @ RT	[116]
Scaffold-assisted process	Toluene	Li_6PS_5Cl + NBR @Nylon membrane	31 - 66	0.18 - 0.55 @ RT	[117]
	Anisole	Li_6PS_5Cl + NBR @laser-driled PI film	27	0.39 @ 27 °C	[118]
	Ethanol	$Li_6PS_5Cl_{0.5}Br_{0.5}$ @PI nonwoven	40 - 70	0.06 - 0.20 @ 30 °C	[119]
	-	Li_6PS_5Cl + Vectran	98	2.9 @ 25 °C	[18]

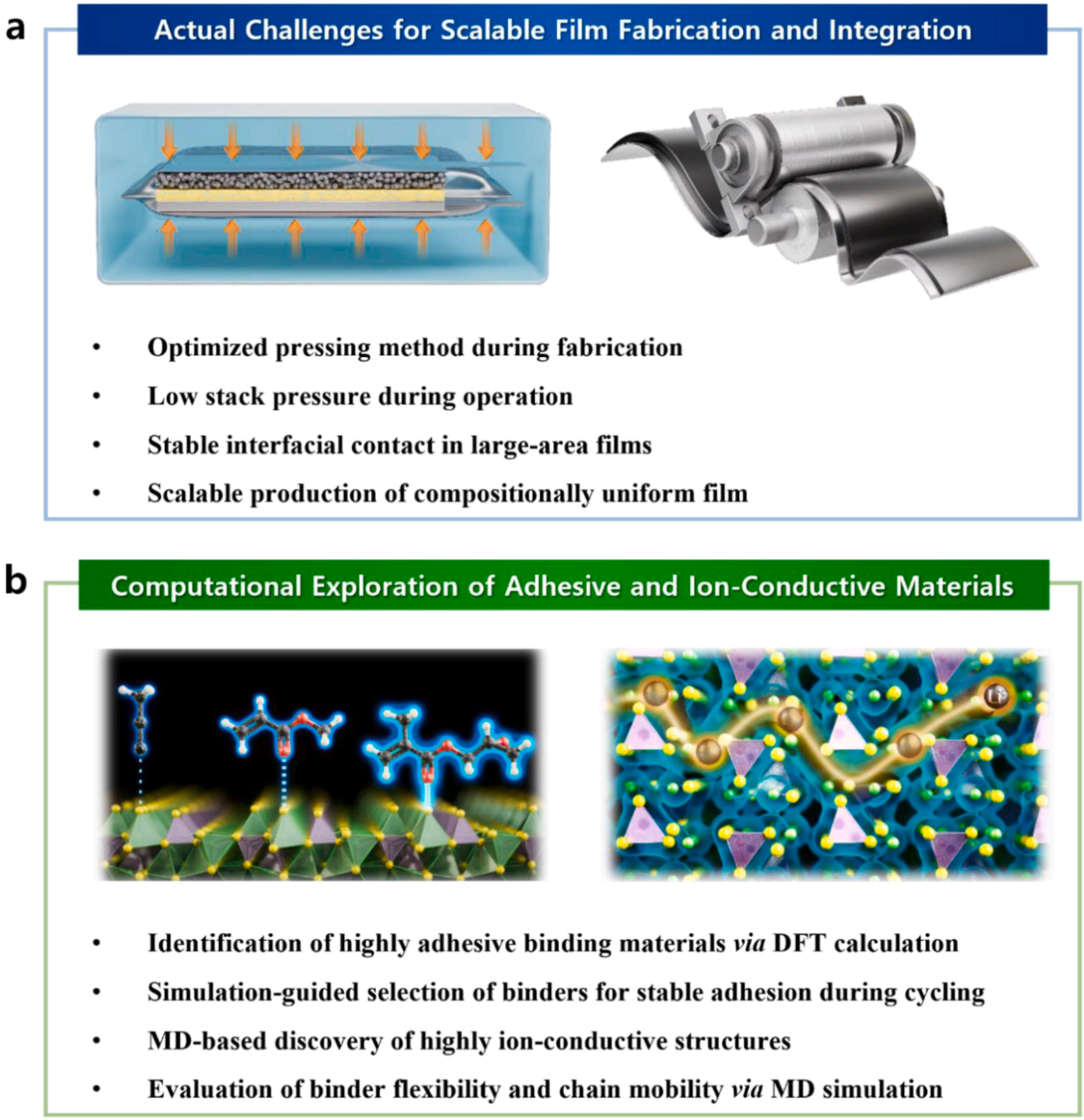

Fig. 10. Schematic illustration of future research directions for (a) scalable ASSLBs film integration and (b) computationally guided polymer binder design.

These factors become increasingly critical at larger scales and are vital for maintaining consistent interfacial adhesion across wide contact areas. Second, intimate inter-film and intra-film contact must be established during the assembly process, even under minimal external pressure. To meet this requirement, polymer binders must provide sufficient adhesiveness and high ionic conductivity under limited pressing conditions. Moreover, films or sheets should achieve the necessary densification and adhesion through conventional roll-pressing techniques, rather than relying on specialized and costly equipment such as warm isostatic pressing systems [125]. These strategies are expected not only to facilitate the fabrication of large-area ASSLBs, but also to enhance their stability under low stack pressures, thereby advancing their successful commercialization.

5.3. Computational approaches

As discussed in previous section, a wide range of variables, particularly those related to binder properties, have been investigated through experimental studies. While experimental data are essential for understanding the relationship between material properties and performance, the complex interactions among polymer structure, composition, and processing parameters make comprehensive experimental testing impractical. To navigate this design space, computational methods such as molecular dynamics (MD) simulations and DFT calculations have emerged as valuable tools. These approaches are increasingly being applied to the development of polymer binders (Fig. 10**b**). For instance, Hong et al. employed DFT calculations to investigate the interactions of methyl acrylate and glycidyl methacrylate groups in the EMG binder with both cathode active materials and solid electrolytes, thereby confirming strong binding characteristics at the interface [55]. In addition, Cha et al. employed DFT calculations to elucidate the strong interfacial adhesion of fluorinated copolymer binder with both active material and solid electrolyte surfaces, revealing enhanced binding energies consistent with its experimentally observed stability [126]. Similarly, Li et al. demonstrated via DFT that poly(vinyl acetate) (PVAC) forms robust Li–O coordination bonds at the PVAC/LPSCl interface, a finding later validated by its high ionic conductivity and mechanical durability [127]. Collectively, these studies demonstrate how theoretical predictions can rationally guide binder design and selection prior to experimental verification. These theoretical analyses corroborated the experimentally observed enhancement in interfacial adhesion. However, these studies did not consider the binder's ability to accommodate the volume fluctuations of active materials, a factor that is also critical for long-term cycling performance. In such cases, the ability to quantitatively predict interfacial degradation and void formation during repeated cycling would provide more direct insights into the practical evaluation of cell performance. This predictive capability is particularly valuable for polymer binders, whose properties are highly dependent on polymer structure, making it impractical to synthesize and experimentally evaluate all possible variations. These challenges highlight the need for advanced computational tools capable of reliably simulating binder performance under realistic electrochemical conditions. In another example, Ponce et al. employed MD simulations to investigate Li^+ ion transport and thermal behavior at the SEI interface [128]. They quantitatively analyzed Li^+ ion hopping through the SEI layer and interfacial speciation induced by electric fields. These atomic-scale analyses provided valuable insights into the structural robustness and ionic conductivity of SEI layers. While the study offers meaningful insights based on a nanoscale model and limited time range, its applicability to more complex battery systems may be inherently constrained. To broaden the predictive capabilities of MD simulations, future research must focus on improving both spatial and temporal resolution through continued methodological advancements. Taken together, DFT- and MD-based strategies are poised to become integral tools for the rational design of polymer binders in ASSLBs. These simulations not only elucidate intrinsic material properties but also enable quantitative prediction of interfacial behavior under realistic cell fabrication conditions. Moving forward, computationally guided methodologies will be essential for refining binder architectures and optimizing interfacial engineering strategies, ultimately enabling the scalable production of high-performance ASSLBs.

6. Conclusion

To accelerate the commercialization of sulfide-based ASSLBs, this article redefines the role of polymer binders from passive mechanical components to active design elements that construct and sustain ion-conductive architectures. While previous research has largely focused on the intrinsic properties of binder materials, we emphasize the necessity of adopting a practical, cell-level approach that prioritizes continuous Li^+ ion conduction alongside mechanical resilience and interfacial compatibility. This paradigm shift calls for binder systems that can serve as integrated ion transport media across composite cathodes, anodes, and solid electrolyte sheets, particularly under low stack pressure, a critical condition for practical pouch and prismatic cell formats. We stress that polymer binder development must be aligned with scalable manufacturing requirements, necessitating properties such as solvent compatibility, compositional uniformity, and low-temperature processability. In addition, the application of computational tools such as DFT and MD simulations is expected to grow. These methods enable predictive modeling of interfacial behavior and transport phenomena, offering atomistic-level insights that inform binder design strategies. Their integration will be crucial for elucidating the complex relationships among polymer chemistry, electrode architecture, and real-world cell performance. Ultimately, this perspective underscores that polymer binders are not secondary components, but key enablers of the electrochemical and mechanical reliability of ASSLBs. By establishing ion-conductive networks and maintaining structural integrity across both electrodes and electrolytes, polymer binders will play a central role in the realization of next-generation ASSLBs technologies.

CRediT authorship contribution statement

Seung-Bo Hong: Writing – original draft, Investigation, Data curation, Conceptualization. **Young-Jun Lee:** Writing – original draft, Investigation, Data curation, Conceptualization. **Hun Kim:** Validation, Investigation. **Min Chang Go:** Investigation, Data curation. **Un-Hyuck Kim:** Writing – review & editing, Supervision, Conceptualization. **Yang-Kook Sun:** Writing – review & editing, Supervision, Conceptualization. **Dong-Won Kim:** Writing – review & editing, Supervision, Funding acquisition, Conceptualization.

Declaration of competing interest

The authors declare that they have no known competing financial interests or personal relationships that could have appeared to influence the work reported in this paper.

Acknowledgments

This work was supported by the National Research Foundation of Korea (RS-2024–00454354, RS-2025–18072968).

Data availability

Data will be made available on request.

References

[1] J. Rogelj, M. d. Elzen, N. Höhne, T. Fransen, H. Fekete, H. Winkler, R. Schaeffer, F. Sha, K. Riahi, M. Meinshausen, Paris agreement climate proposals need a boost to keep warming well below 2 °C, Nature 534 (2016) 631–639, https://doi.org/10.1038/nature18307.

[2] Z. Yang, H. Huang, F. Lin, Sustainable electric vehicle batteries for a sustainable world: perspectives on battery cathodes, environment, supply chain, manufacturing, life cycle, and policy, Adv. Energy Mater. 12 (2022) 2200383, https://doi.org/10.1002/aenm.202200383.

[3] M. Dixit, B. Witherspoon, N. Muralidharan, M.M. Mench, C.-B.M. Kweon, Y.-K. Sun, I. Belharouak, Insights into the critical materials supply chain of the battery market for enhanced energy security, ACS Energy Lett. 9 (2024) 3780–3789, https://doi.org/10.1021/acsenergylett.4c01300.

[4] K. Liu, Y. Liu, D. Lin, A. Pei, Y. Cui, Materials for lithium-ion battery safety, Sci. Adv. 4 (2018) eaas9820, https://doi.org/10.1126/sciadv.aas9820.

[5] X. Feng, M. Ouyang, X. Liu, L. Lu, Y. Xia, X. He, Thermal runaway mechanism of lithium ion battery for electric vehicles: a review, Energy Storage Mater. 10 (2018) 246–267, https://doi.org/10.1016/j.ensm.2017.05.013.

[6] Y.-K. Sun, Promising all-solid-state batteries for future electric vehicles, ACS Energy Lett. 5 (2020) 3221–3223, https://doi.org/10.1021/acsenergylett.0c01977.

[7] Y. Kato, S. Hori, T. Saito, K. Suzuki, M. Hirayama, A. Mitsui, M. Yonemura, H. Iba, R. Kanno, High-power all-solid-state batteries using sulfide superionic conductors, Nat. Energy 1 (2016) 16030, https://doi.org/10.1038/nenergy.2016.30.

[8] J. Lau, R.H. DeBlock, D.M. Butts, D.S. Ashby, C.S. Choi, B.S. Dunn, Sulfide solid electrolytes for lithium battery applications, Adv. Energy Mater. 8 (2018) 1800933, https://doi.org/10.1002/aenm.201800933.

[9] J. Wu, S. Liu, F. Han, X. Yao, C. Wang, Lithium/Sulfide all-solid-state batteries using sulfide electrolytes, Adv. Mater. 33 (2021) 2000751, https://doi.org/10.1002/adma.202000751.

[10] A. Banerjee, X. Wang, C. Fang, E.A. Wu, Y.S. Meng, Interfaces and interphases in all-solid-state batteries with inorganic solid electrolytes, Chem. Rev. 120 (2020) 6878–6933, https://doi.org/10.1021/acs.chemrev.0c00101.

[11] S.-B. Hong, Y.-J. Lee, H.-J. Lee, H.-T. Sim, H. Lee, Y.M. Lee, D.-W. Kim, Exploring the cathode active materials for sulfide-based all-solid-state lithium batteries with high energy density, Small 20 (2024) 2304747, https://doi.org/10.1002/smll.202304747.

[12] Y.-Q. Zhang, Y. Tian, Y. Xiao, L.-J. Miara, Y. Aihara, T. Tsujimura, T. Shi, M. C. Scott, G. Ceder, Direct visualization of the interfacial degradation of cathode coatings in solid state batteries: a combined experimental and computational study, Adv. Energy Mater. 10 (2023) 1903778, https://doi.org/10.1002/aenm.201903778.

[13] K.T. Kim, J. Woo, Y.-S. Kim, S. Sung, C. Park, C. Lee, Y.J. Park, H.-W. Lee, K. Park, Y.S. Jung, Ultrathin superhydrophobic coatings for air-stable inorganic solid electrolytes: toward dry room application for all-solid-state batteries, Adv. Energy Mater. 13 (2023) 2301600, https://doi.org/10.1002/aenm.202301600.

[14] F. Zhao, J. Liang, C. Yu, Q. Sun, X. Li, K. Adair, C. Wang, Y. Zhao, S. Zhang, W. Li, S. Deng, R. Li, Y. Huang, H. Huang, L. Zhang, S. Zhao, S. Lu, X. Sun, A versatile sn-substituted argyrodite sulfide electrolyte for all-solid-state Li metal batteries, Adv. Energy Mater. 10 (2020) 1903422, https://doi.org/10.1002/aenm.201903422.

[15] H.-S. Kim, S. Park, S. Kang, J.Y. Jung, K. Kim, J.-S. Yu, D.-W. Kim, J.-W. Lee, Y.-K. Sun, W. Cho, Accelerated degradation of all-solid-state batteries induced through volumetric occupation of the carbon additive in the solid electrolyte domain, Adv. Funct. Mater. 34 (2024) 2409318, https://doi.org/10.1002/adfm.202409318.

[16] Y.B. Song, K.H. Baeck, H. Kwak, H. Lim, Y.S. Jung, Dimensional strategies for bridging the research gap between lab-scale and potentially practical all-solid-state batteries: the role of sulfide solid electrolyte films, Adv. Energy Mater. 13 (2023) 2301142, https://doi.org/10.1002/aenm.202301142.

[17] J. Park, K.T. Kim, D.Y. Oh, D. Jin, D. Kim, Y.S. Jung, Y.M. Lee, Digital twin-driven all-solid-state battery: unraveling the physical and electrochemical behaviors, Adv. Energy Mater. 10 (2020) 2001536, https://doi.org/10.1002/aenm.202001563.

[18] S.-E. Lee, H.-T. Sim, Y.-J. Lee, S.-B. Hong, K.Y. Chung, H.-G. Jung, D.-W. Kim, Li_6PS_5Cl-based composite electrolyte reinforced with high-strength polyester fibers for all-solid-state lithium batteries, J. Power Sources 542 (2022) 536–542, https://doi.org/10.1016/j.jpowsour.2022.231777.

[19] J.Y. Kim, J. Park, M.J. Lee, S.H. Kang, D.O. Shin, J. Oh, J. Kim, K.M. Kim, Y.-G. Lee, Y.M. Lee, Diffusion-Dependent graphite electrode for all-solid-state batteries with extremely high energy density, ACS Energy Lett. Mater. 5 (2020) 2995–3004, https://doi.org/10.1021/acsenergylett.0c01628.

[20] S. Cho, Y. Kim, Y. Song, J. Ryu, K. Choi, J. Yang, S.-H. Lee, S.G. Im, S. Park, Functional polymer thin films for establishing an effective electrode interface in sulfide-based solid-state batteries, Adv. Funct. Mater. 34 (2024) 2314710, https://doi.org/10.1002/adfm.202314710.

[21] T. Dai, S. Wu, Y. Lu, Y. Yang, Y. Liu, C. Chang, X. Rong, R. Xiao, J. Zhao, Y. Liu, W. Wang, L. Chen, Y.-S. Hu, Inorganic glass electrolytes with polymer-like viscoelasticity, Nat. Energy 8 (2023) 1221–1228, https://doi.org/10.1038/s41560-023-01356-y.

[22] D.H.S. Tan, Y.S. Meng, J. Jang, Scaling up high-energy-density sulfidic solid-state batteries: a lab-to-pilot perspective, Joule 6 (2022) 1755–1769, https://doi.org/10.1016/j.joule.2022.07.002.

[23] H. Lim, S. Jun, Y.B. Song, H. Bae, J.H. Kim, Y.S. Jung, Operando electrochemical pressiometry probing interfacial evolution of electrodeposited thin lithium metal anodes for all-solid-state batteries, Energy Storage Mater. 50 (2022) 543–553, https://doi.org/10.1016/j.ensm.2022.05.050.

[24] N.-Y. Park, H.-U. Lee, T.-Y. Yu, I.-S. Lee, H. Kim, S.-M. Park, H.-G. Jung, Y.-C. Jung, Y.-K. Sun, High-energy, long-life ni-rich cathode materials with columnar structures for all-solid-state batteries, Nat. Energy 10 (2025) 479–489, https://doi.org/10.1038/s41560-025-01726-8.

[25] S.H. Jung, U.-H. Kim, J.-H. Kim, S. Jun, C.S. Yoon, Y.S. Jung, Y.-K. Sun, Ni-Rich layered cathode materials with electrochemo-mechanically compliant microstructures for all-solid-state li batteries, Adv. Energy Mater. 10 (2020) 1993360, https://doi.org/10.1002/aenm.201903360.

[26] T.-Y. Yu, N.-Y. Park, H. Kim, I.-S. Lee, H.-U. Lee, K.-H. Kim, W. Cho, H.-G. Jung, K. Y. Chung, Y.-K. Sun, Tuning the lithium diffusion kinetics in co-free layered cathodes for high-performance all-solid-state batteries, ACS Energy Lett. 10 (2025) 2477–2486, https://doi.org/10.1021/acsenergylett.5c00961.

[27] U.-H. Kim, T.-Y. Yu, J.W. Lee, H.U. Lee, I. Belharouak, C.S. Yoon, Y.-K. Sun, Microstructure- and Interface-Modified Ni-rich cathode for high-energy-density all-solid-state lithium batteries, ACS Energy Lett 8 (2023) 809–817, https://doi.org/10.1021/acsenergylett.2c02715.

[28] D. Lee, Y. Shim, Y. Kim, G. Kwon, S.H. Choi, K. Kim, D.-J. Yoo, Shear force effect of the dry process on cathode contact coverage in all-solid-state batteries, Nat. Commun. 15 (2024) 4763. https://http://doi.org/10.1038/s41467-024-49183-3.

[29] K. Lee, S. Kim, J. Park, S.H. Park, A. Coskun, D.S. Jung, W. Cho, J.W. Choi, Selection of binder and solvent for solution-processed all-solid-state battery, J. Electrochem. Soc. 164 (2017) A2075, https://doi.org/10.1149/2.1341709jes.

[30] Y.J. Nam, D.Y. Oh, S.H. Jung, Y.S. Jung, Toward practical all-solid-state lithium-ion batteries with high energy density and safety: comparative study for electrodes fabricated by dry- and slurry-mixing processes, J. Power Sources 375 (2018) 93–101, https://doi.org/10.1016/j.jpowsour.2017.11.031.

[31] X. Wang, L. Ye, C.-W. Nan, X. Li, Effect of solvents on a $Li_{10}GeP_2S_{12}$-Based composite electrolyte via solution method for solid-state battery applications, ACS Appl. Mater. Interfaces 14 (2022) 46627–46636, https://doi.org/10.1021/acsami.2c12920.

[32] A. Altvater, J. Klemens, J. Borho, A. Smith, T. Heckmann, P. Scharfer, W. Schabel, Application of multistage drying profiles for accelerated production of li-ion battery anodes using infrared radiation: validation with electrochemical performance and structural properties, Energy Technol. 12 (2024) 2301272, https://doi.org/10.1002/ente.202301272.

[33] N. Kumano, Y. Yamaguchi, Y. Akimoto, A. Ohshima, H. Nakamura, M. Yamamura, Migration of binder and conductive agent during drying process of li-ion battery cathodes, J. Power Sources 591 (2024) 233883, https://doi.org/10.1016/j.jpowsour.2023.233883.

[34] K.-Y. Park, J.-W. Park, W.M. Seong, K. Yoon, T.-H. Hwang, K.-H. Ko, J.-H. Han, Y. Jaedong, K. Kang, Understanding capacity fading mechanism of thick electrodes for lithium-ion rechargeable batteries, J. Power Sources 468 (2020) 228369, https://doi.org/10.1016/j.jpowsour.2020.228369.

[35] Y. Nomura, K. Yamamoto, T. Hirayama, E. Igaki, K. Saitoh, Visualization of lithium transfer resistance in secondary particle cathodes of bulk-type solid-state batteries, ACS Energy Lett 5 (2020) 2098–2105, https://doi.org/10.1021/acsenergylett.0c00942.

[36] J.K. Koo, J. Lim, J. Shin, J.K. Seo, C. Ha, W.T.A. Ran, J.-H. Lee, Y. Kwon, Y. M. Lee, Y.-J. Kim, Dry-processed ultra-high-energy cathodes (99.6wt%, 4.0 g cm^{-3}) using single-crystalline ni-rich oxides, Energy Storage Mater 78 (2025) 104270, https://doi.org/10.1016/j.ensm.2025.104270.

[37] F. Hippauf, B. Schumm, S. Doerfler, H. Althues, S. Fujiki, T. Shiratsuchi, T. Tsujimura, Y. Aihara, S. Kaskel, Overcoming binder limitations of sheet-type solid-state cathodes using a solvent-free dry-film approach, Energy Storage Mater. 21 (2019) 390–398, https://doi.org/10.1016/j.ensm.2019.05.033.

[38] K. Lee, Y. Jo, J.S. Nam, H. Yu, Y.-J. Kim, Dry-film technology employing cryo-pulverized polytetrafluoroethylene binder for all-solid-state batteries, Chem. Eng. J. 487 (2024) 150221, https://doi.org/10.1016/j.cej.2024.150221.

[39] D. Lee, A. Manthiram, Stable cycling with intimate contacts enabled by crystallinity-controlled PTFE-Based solvent-free cathodes in all-solid-state batteries, Small Methods 7 (2023) 2201680, https://doi.org/10.1002/smtd.202201680.

[40] Y.-J. Lee, S.-Y. Kim, W.-J. Song, J. Cha, D.-W. Kim, Enhancing the cycling performance of sulfide-based all-solid-state lithium batteries via molecular weight-dependent fibrillation of ptfe binders, Mater. Today Energy 51 (2025) 101914, https://doi.org/10.1016/j.mtener.2025.101914.

[41] T.Y. Kwon, K.T. Kim, D.Y. Oh, Y.B. Song, S. Jun, Y.S. Jung, Three-dimensional networking binders prepared in situ during wet-slurry process for all-solid-state batteries operating under low external pressure, Energy Storage Mater. 49 (2022) 219–226, https://doi.org/10.1016/j.ensm.2022.04.017.

[42] J. Lee, K. Lee, T. Lee, H. Kim, K. Kim, W. Cho, A. Coskun, K. Char, J.W. Choi, In situ deprotection of polymeric binders for solution-processible sulfide-based all-solid-state batteries, Adv. Mater. 32 (2020) 2001702, https://doi.org/10.1002/adma.202001702.

[43] K. Lee, J. Lee, S. Choi, K. Char, J.W. Choi, Thiol–Ene click reaction for fine polarity tuning of polymeric binders in solution-processed all-solid-state batteries, ACS Energy Lett 4 (2019) 94–101, https://doi.org/10.1021/acsenergylett.8b01726.

[44] M.P. Lautenschlaeger, B. Prifling, B. Kellers, J. Weinmiler, T. Danner, V. Schmidt, A. Latz, Understanding electrolyte filling of lithium-ion battery electrodes on the pore scale using the lattice boltzmann method, Batteries Supercaps 5 (2022) e202200090, https://doi.org/10.1002/batt.202200090.

[45] H.-S. Kim, J.Y. Jung, K. Kim, C. Hwang, J. Yu, M.-S. Park, W. Cho, Functionalized electrode additive for simultaneously reinforcing chemo-mechanical properties of millimeter-thick dry-electrode for high-energy all-solid-state batteries, Adv. Energy Mater. 14 (2024) 2303965, https://doi.org/10.1002/aenm.202303965.

[46] K.-J. Lee, Y.-W. Byeon, H.-J. Lee, Y. Lee, S. Park, H.-R. Kim, H.-K. Kim, S.J. Oh, J.-P. Ahn, Revealing crack-healing mechanism of NCM composite cathode for sustainable cyclability of sulfide-based solid-state batteries, Energy Storage Mater. 57 (2023) 326–333, https://doi.org/10.1016/j.ensm.2023.01.012.

[47] S.-B. Hong, Y.-J. Lee, U.-H. Kim, C. Bak, Y.M. Lee, W. Cho, H.J. Hah, Y.-K. Sun, D.-W. Kim, All-Solid-State lithium batteries: Li^+-Conducting ionomer binder for dry-processed composite cathodes, ACS Energy Lett 7 (2022) 1092–1100, https://doi.org/10.1021/acsenergylett.1c02756.

[48] L. Tian, J.-W. Kim, D.-W. Kim, Solid hybrid electrolytes based on conductive oxides and polymer electrolytes for all-solid-lithium batteries, Mater. Chem. Front. 8 (2024) 455–484, https://doi.org/10.1039/D3QM00736G.

[49] T. Yang, J. Zheng, Q. Cheng, Y.-Y. Hu, C.K. Chan, ACS Appl. Mater. Interfaces 9 (2017) 21773–21780, https://doi.org/10.1021/acsami.7b03806.

[50] S. Sen, E. Trevisanello, E. Niemöller, B.-X. Shi, F.J. Simon, F.H. Richter, J. Mater. Chem. A 9 (2021) 18701–18732, https://doi.org/10.1039/D1TA02796D.

[51] J. Cha, S. Kim, U.T. Nakate, D.-W. Kim, Highly conductive composite cathode prepared by dry process using NAFION-Li ionomer for sulfide-based all-solid-state lithium batteries, J. Power Sources 613 (2024) 234914, https://doi.org/10.1016/j.jpowsour.2024.234914.

[52] T. Charlesworth, K. Yiamsawat, H. Gao, G.J. Rees, C.K. Williams, P.G. Bruce, M. Pasta, G.L. Gregory, Lithium borate polycarbonates for high-capacity solid-state composite cathodes, Angew. Chem. Int. Ed. 63 (2024) e202408246, https://doi.org/10.1002/anie.202408246.

[53] D.Y. Oh, Y.J. Nam, K.H. Park, S.H. Jung, K.T. Kim, A.R. Ha, Y.S. Jung, Slurry-Fabricable li^+-conductive polymeric binders for practical all-solid-state lithium-ion batteries enabled by solvate ionic liquids, Adv. Energy Mater. 9 (2019) 1802927, https://doi.org/10.1002/aenm.201802927.

[54] D.Y. Oh, K.T. Kim, S.H. Jung, D.H. Kim, S. Jun, S. Heoung, H.R. Moon, Y.S. Jung, Tactical hybrids of Li^+-conductive dry polymer electrolytes with sulfide solid electrolytes: toward practical all-solid-state batteries with wider temperature operability, Mater. Today 53 (2022) 2400802, https://doi.org/10.1016/j.mattod.2021.01.006.

[55] S.-B. Hong, Y.-R. Jang, H. Kim, Y.-C. Jung, G. Shin, H.J. Hah, W. Cho, Y.-K. Sun, D.-W. Kim, Wet-Processable binder in composite cathode for high energy density all-solid-state lithium batteries, Adv. Energy Mater. 14 (2024) 2400802, https://doi.org/10.1002/aenm.202400802.

[56] E. Stefanis, C. Panayiotou, Prediction of hansen solubility parameters with a new group-contribution method, Int. J. Thermophys. 29 (2008) 568–585, https://doi.org/10.1007/s10765-008-0415-z.

[57] K.T. Kim, D.Y. Oh, S. Jun, Y.B. Song, T.Y. Kwon, Y. Han, Y.S. Jung, Tailoring slurries using cosolvents and Li salt targeting practical all-solid-state batteries employing sulfide solid electrolytes, Adv. Energy Mater. 11 (2021) 2003766, https://doi.org/10.1002/aenm.202003766.

[58] D. Ren, L. Lu, R. Hua, G. Zhu, X. Liu, Y. Mao, X. Rui, S. Wang, B. Zhao, H. Cui, M. Yang, H. Shen, C.-Z. Zhao, L. Wang, X. He, S. Liu, U. Hou, T. Tan, P. Wang, Y. Nitta, M. Ouyang, Challenges and opportunities of practical sulfide-based all-solid-state batteries, eTransportation 18 (2023) 100272, https://doi.org/10.1016/j.etran.2023.100272.

[59] H. Huo, J. Janek, Silicon as emerging anode in solid-state batteries, ACS Energy Lett. 7 (2022) 4005–4016, https://doi.org/10.1021/acsenergylett.2c01950.

[60] Q. Sun, G. Zeng, X. Xu, J. Li, J.J. Biendicho, S. Wang, Y. Tian, L. Ci, A. Cabot, Are sulfide-based solid-state electrolytes the best pair for Si anodes in Li-ion batteries? Adv. Energy Mater. 14 (2024) 2402048 https://doi.org/10.1002/aenm.202402048.

[61] P. Oh, J. Yun, J.H. Choi, K.S. Saqib, T.J. Embleton, S. Park, C. Lee, J. Ali, K. Ko, J. Cho, Development of high-energy anodes for all-solid-state lithium batteries based on sulfide electrolytes, Angew. Chem. Int. Ed. 61 (2022) e202201249, https://doi.org/10.1002/anie.202201249.

[62] J. Wang, H. Zhu, Sulfide-Based anode-free solid-state batteries: key challenges and emerging solutions, ACS Energy Lett. 10 (2025) 2377–2391, https://doi.org/10.1021/acsenergylett.5c00517.

[63] D. Cao, T. Ji, A. Singh, S. Bak, Y. Du, X. Xiao, H. Xu, J. Zhu, H. Zhu, Unveiling the mechanical and electrochemical evolution of nanosilicon composite anodes in sulfide-based all-solid-state batteries, Adv. Energy Mater. 13 (2023) 2203969, https://doi.org/10.1002/aenm.202203969.

[64] M. Otoyama, N. Terasaki, T. Takeuchi, T. Okumura, K. Kuratani, Visualization of local strain distributions in all-solid-state batteries with silicon negative electrodes using digital image correlation for operando/in situ microscopy images, ChemElectroChem 12 (2013) 18600–18606, https://doi.org/10.1002/celc.202400616.

[65] M. Nagao, A. Hayashi, M. Tatsumisago, T. Kanetsuku, T. Tsuda, S. Kuwabata, In situ SEM study of a lithium deposition and dissolution mechanism in a bulk-type solid-state cell with a Li_2S–P_2S_5 solid electrolyte, Phys. Chem. Chem. Phys. 15 (2013) 18600–18606, https://doi.org/10.1039/C3CP51059J.

[66] J. Liu, H. Yuan, H. Liu, C.-Z. Zhao, Y. Lu, X.-B. Cheng, J.-Q. Huang, Q. Zhang, Unlocking the failure mechanism of solid state lithium metal batteries, Adv. Energy Mater. 12 (2022) 2100748, https://doi.org/10.1002/aenm.202100748.

[67] Z. Zhang, J. Wang, Y. Jin, G. Liu, S. Yang, X. Yao, Insights on lithium plating behavior in graphite-based all-solid-state lithium-ion batteries, Energy Storage Mater 54 (2023) 845–853, https://doi.org/10.1016/j.ensm.2022.11.023.

[68] S. Yang, K. Yamamoto, X. Mei, A. Sakuda, T. Uchiyama, T. Watanabe, T. Takami, A. Hayashi, M. Tatsumisago, Y. Uchimoto, High rate capability from a graphite anode through surface modification with lithium iodide for all-solid-state batteries, ACS Appl. Energy Mater. 5 (2022) 667–673, https://doi.org/10.1021/acsaem.1c03166.

[69] D.O. Shin, H. Kim, S. Jung, S. Byun, J. Choi, M.P. Kim, J.Y. Kim, S.H. Kang, Y.-S. Park, S.Y. Hong, M. Cho, Y.-G. Lee, K. Cho, Y.M. Lee, Electrolyte-free graphite electrode with enhanced interfacial conduction using Li^+-conductive binder for high-performance all-solid-state batteries, Energy Storage Mater 49 (2022) 481–492, https://doi.org/10.1016/j.ensm.2022.04.029.

[70] D.H.S. Tan, Y.-T. Chen, H. Yang, W. Bao, B. Sreenarayanan, J.-M. Doux, W. Li, B. Lu, S.-Y. Ham, B. Sayahpour, J. Scharf, E.A. Wu, G. Deysher, H.E. Han, H. J. Hah, H. Jeong, J.B. Lee, Z. Chen, Y.S. Meng, Carbon-free high-loading silicon anodes enabled by sulfide solid electrolytes, Science 373 (2021) 1494–1499, https://doi.org/10.1126/science.abg7217.

[71] D. Cao, X. Sun, Y. Li, A. Anderson, W. Lu, H. Zhu, Long-Cycling sulfide-based all-solid-state batteries enabled by electrochemo-mechanically stable electrodes, Adv. Mater. 34 (2022) 2200401, https://doi.org/10.1002/adma.202200401.

[72] W. Ping, C. Yang, Y. Bao, C. Wang, H. Xie, E. Hitz, J. Cheng, T. Li, L. Hu, A silicon anode for garnet-based all-solid-state batteries: interfaces and nanomechanics, Energy Storage Mater 21 (2019) 246–252, https://doi.org/10.1016/j.ensm.2019.06.024.

[73] M. Grandjean, M. Pichardo, Y. Biecher, C. Haon, P. Chenevier, Matching silicon-based anodes with sulfide-based solid-state electrolytes for Li-ion batteries, J. Power Source 580 (2023) 233386, https://doi.org/10.1016/j.jpowsour.2023.233386.

[74] S. Jing, Y. Lu, Y. Huang, H. Liu, Y. Shen, W. Kuang, H. Shen, S. Liu, Z. Zhang, F. Liu, High-Performance sheet-type sulfide all-solid-state batteries enabled by dual-function $Li_{4.4}Si$ alloy-modified nano silicon anodes, Adv. Mater. 36 (2024) 2312305, https://doi.org/10.1002/adma.202312305.

[75] Y. Huang, S. Jing, H. Shen, S. Li, Y. Shen, Y. Lin, Y. Zhang, Z. Zhang, Y. Liu, Y. Chen, F. Liu, Y. Lu, An electrochemical-mechanical synergistic regulation by constructing a double-layer fully active silicon-based alloy anode in sulfide all-solid-state batteries, Acta Mater. 289 (2025) 120915, https://doi.org/10.1016/j.actamat.2025.120915.

[76] W. Yan, Z. Mu, Z. Wang, Y. Huang, D. Wu, P. Lu, J. Lu, J. Xu, Y. Wu, T. Ma, M. Yang, X. Zhu, Y. Xai, S. Shi, L. Chen, H. Li, F. Wu, Hard-carbon-stabilized li–si anodes for high-performance all-solid-state Li-ion batteries, Nat. Energy 8 (2023) 800–813, https://doi.org/10.1038/s41560-023-01279-8.

[77] J. Moon, H.C. Lee, H. Jung, S. Wakita, S. Cho, J. Yoon, J. Lee, A. Ueda, B. Choi, S. Lee, K. Ito, Y. Kubo, A.C. Lim, J.G. Seo, J. Yoo, S. Lee, Y. Ham, W. Baek, Y.-G. Ryu, I.T. Han, Interplay between electrochemical reactions and mechanical responses in silicon–graphite anodes and its impact on degradation, Nat. Commun. 12 (2021) 2714, https://doi.org/10.1038/s41467-021-22662-7.

[78] Y.J. Nam, K.H. Park, D.Y. Oh, W.H. An, Y.S. Jung, Diagnosis of failure modes for all-solid-state Li-ion batteries enabled by three-electrode cells, J. Mater. Chem. A 6 (2018) 14867–14875, https://doi.org/10.1039/C8TA03450H.

[79] J. Kim, J. Jeong, D. Lee, J. Kim, M. Naito, H. Park, T. Song, U. Paik, Rational material design on high capacity and long-term-cyclability of graphite/Si-based anodes for room temperature all-solid-state batteries, Chem. Eng. J. 505 (2025) 159328, https://doi.org/10.1016/j.cej.2025.159328.

[80] J. Choi, C. Bak, J.Y. Kim, D.O. Shin, S.H. Kang, Y.M. Lee, Y.-G. Lee, Enhancing electrochemo-mechanical properties of graphite-silicon anode in all-solid-state batteries via solvent-induced polar interactions in nitrile binders, J. Energy Chem. 105 (2025) 514–524, https://doi.org/10.1016/j.jechem.2025.02.012.

[81] Y. Nikodimos, C.-J. Huang, B.W. Taklu, W.-N. Su, B.J. Hwang, Chemical stability of sulfide solid-state electrolytes: stability toward humid air and compatibility with solvents and binders, Energy Environ. Sci. 15 (2022) 991–1033, https://doi.org/10.1039/D1EE03032A.

[82] J. Oh, S.H. Choi, H. Kim, W.J. Chung, M. Kim, I. Kim, T. Lee, J. Lee, D.O. Kim, S. Moon, D. Kim, J.W. Choi, Solvent–Binder engineering for a practically viable solution process for fabricating sulfide-based all-solid-state batteries, ACS Energy Lett 6 (2025) 2831–2838, https://doi.org/10.1021/acsenergylett.5c00762.

[83] W. Xu, J. Wang, F. Ding, X. Chen, E. Nasybulin, Y. Zhang, J.-G. Zhang, Lithium metal anodes for rechargeable batteries, Energy Environ. Sci. 7 (2014) 513–537, https://doi.org/10.1039/C3EE40795K.

[84] W.D. Richards, L.J. Miara, Y. Wang, J.C. Kim, G. Ceder, Interface stability in solid-state batteries, Chem. Mater. 28 (2016) 266–273, https://doi.org/10.1021/acs.chemmater.5b04082.

[85] J. Kasemchainan, S. Zekoll, D.S. Jolly, Z. Ning, G.O. Hartley, J. Marrow, P. G. Bruce, Critical stripping current leads to dendrite formation on plating in lithium anode solid electrolyte cells, Nat. Mater. 18 (2019) 1105–1111, https://doi.org/10.1038/s41563-019-0438-9.

[86] X. Ji, S. Hou, P. Wang, X. He, N. Piao, J. Chen, X. Fan, C. Wang, Solid-State electrolyte design for lithium dendrite suppression, Adv. Mater. 32 (2020) 2002741, https://doi.org/10.1002/adma.202002741.

[87] M. Wu, M. Li, Y. Jin, X. Chang, X. Zhao, Z. Gu, G. Liu, X. Yao, In situ formed LiF-Li_3N interface layer enables ultra-stable sulfide electrolyte-based all-solid-state lithium batteries, J. Energy Chem. 79 (2023) 272–278, https://doi.org/10.1016/j.jechem.2023.01.007.

[88] Y.-E. Park, M.-K. Oh, H.-T. Sim, H.-J. Kim, Y.-S. Cho, S.-J. Park, D.-W. Kim, Rationally designed li–ag alloy with in-situ-formed solid electrolyte interphase for all-solid-state lithium batteries, ACS Appl. Mater. Interfaces 16 (2024) 39460–39469, https://doi.org/10.1021/acsami.4c08541.

[89] H. Su, Y. Liu, Y. Zhong, J. Li, X. Wang, X. Xia, C. Gu, J. Tu, Stabilizing the interphase between Li and argyrodite electrolyte through synergistic phosphating process for all-solid-state lithium batteries, Nano Energy 96 (2022) 107104, https://doi.org/10.1016/j.nanoen.2022.107104.

[90] H.-T. Sim, M.-K. Oh, H.-J. Kim, Y.-E. Park, Y.-S. Cho, J. Choi, S.-J. Park, D.-W. Kim, Surface-Modified lithium enabling high-performance all-solid-state lithium metal batteries, ACS Energy Lett. 10 (2025) 2277–2284, https://doi.org/10.1021/acsenergylett.5c00656.

[91] J.-M. Doux, H. Nguyen, D.H.S. Tan, A. Banerjee, X. Wang, E.A. Wu, C. Jo, H. Yang, Stack pressure considerations for room-temperature all-solid-state lithium metal batteries, Adv. Energy Mater. 10 (2020) 1903253, https://doi.org/10.1002/aenm.201903253.

[92] C. Hänsel, D. Kundu, The stack pressure dilemma in sulfide electrolyte based li metal solid-state batteries: a case study with Li_6PS_5Cl solid electrolyte, Adv. Mater. Interfaces 8 (2021) 2100206, https://doi.org/10.1002/admi.202100206.

[93] S.-J. Jeon, U.-H. Kim, S.H. Kwag, J.-W. Min, D.-W. Kim, H. Kim, All-Solid-State batteries with anodeless electrodes: research trend and future perspective, Adv. Mater. Interfaces 12 (2025) 2400953, https://doi.org/10.1002/admi.202400953.

[94] F. Xie, M.S. Diallo, H. Kim, Q.H. Tu, G. Ceder, The microscopic mechanism of lithiation and delithiation in the Ag/C buffer layer for anode-free solid-state batteries, Adv. Energy Mater. 14 (2024) 2320960, https://doi.org/10.1002/aenm.202302960.

[95] Y.-G. Lee, S. Fujiki, C. Jung, N. Suzuki, N. Yashiro, R. Omoda, D.-S. Ko, T. Shiratsuchi, T. Sugimoto, S. Ryu, J.H. Ku, T. Watanabe, Y. Park, Y. Aihara, D. Im, I.T. Han, High-energy long-cycling all-solid-state lithium metal batteries enabled by silver–carbon composite anodes, Nat. Energy 5 (2020) 299–308, https://doi.org/10.1038/s41560-020-0575-z.

[96] J. Oh, S.H. Choi, B. Chang, J. Lee, T. Lee, N. Lee, H. Kim, Y. Kim, G. Im, S. Lee, J. W. Choi, Elastic binder for high-performance sulfide-based all-solid-state batteries, ACS Energy Lett 7 (2022) 1374–1382, https://doi.org/10.1021/acsenergylett.2c00461.

[97] J. Lee, S.H. Choi, G. Im, K.-J. Lee, T. Lee, J. Oh, N. Lee, H. Kim, Y. Kim, S. Lee, J. W. Choi, Room-Temperature anode-less all-solid-state batteries via the conversion reaction of metal fluorides, Adv. Mater. 34 (2022) 2203580, https://doi.org/10.1002/adma.202203580.

[98] D. Jun, S.H. Park, J.E. Jung, S.G. Lee, K.S. Kim, J.Y. Kim, K.Y. Bae, S. Son, Y. J. Lee, Ultra-Stable breathing anode for li-free all-solid-state battery based on li concentration gradient in magnesium particles, Adv. Funct. Mater. 34 (2024) 2310259, https://doi.org/10.1002/adfm.202310259.

[99] S.-J. Jeon, C. Hwang, H.-S. Kim, J. Park, J.-Y. Hwang, Y. Jung, R. Choi, M.-S. Song, Y.J. Lee, J.-S. Yu, Y.-C. Jung, Sonochemically prepared nanodot magnesium fluoride-based anodeless carbon substrate for simultaneously reinforcing interphasial and reaction kinetics for sulfide-based all-solid-state batteries, Adv. Energy Mater. 14 (2024) 2408227, https://doi.org/10.1002/aenm.202402887.

[100] J. Oh, S.H. Choi, H. Kim, J.Y. Kim, G.-J. Lee, K.Y. Bae, T. Lee, N. Lee, Y. Sohn, W. J. Chung, J.W. Choi, Lithio-amphiphilic nanobilayer for high energy density anode-less all-solid-state batteries operating under low stack pressure, Energy Environ. Sci. 17 (2024) 7932–7943, https://doi.org/10.1039/D4EE03130J.

[101] J. Oh, S.H. Choi, J.Y. Kim, J. Lee, T. Lee, N. Lee, T. Lee, Y. Sohn, W.J. Chung, K. Y. Bae, S. Son, J.W. Choi, Anode-Less all-solid-state batteries operating at room temperature and low pressure, Adv. Energy Mater. 13 (2023) 2301508, https://doi.org/10.1002/aenm.202301508.

[102] J. Oh, Y. Sohn, J.W. Choi, High-performance anode-less all-solid-state batteries enabled by multisite nucleation and an elastic network, EES Batteries 1 (2025) 566–575, https://doi.org/10.1039/D5EB00050E.

[103] G. Maresca, A. Tsurumaki, N. Suzukui, T. Tsujimura, Y. Aihara, M.A. Navarra, Improvement of graphite interfacial stability in all-solid-state cells adopting sulfide glassy electrolytes, ChemElectroChem 9 (2024) 689–698, https://doi.org/10.1002/celc.202001291.

[104] H.-J. Lee, H.-R. Kim, K.-J. Lee, Y. Lee, H.-K. Kim, W.-Y. Yoon, J.-P. Ahn, Crack healing mechanism by application of stack pressure to the carbon-based composite anode of an all-solid-state battery, ACS Appl. Energy Mater. 5 (2022) 5227–5235, https://doi.org/10.1021/acsaem.2c00603.
[105] G. Wang, A. Mijailovic, J. Yang, J. Xiong, S.E. Beasley, K. Mathew, B. Zhou, W. Lu, B.W. Sheldon, Q. Wu, Particle size effect of graphite anodes on performance of fast charging li-ion batteries, J. Mater. Chem. A 11 (2023) 21793–21805, https://doi.org/10.1039/D3TA00608E.
[106] H. Huo, M. Jiang, Y. Bai, S. Ahmed, K. Volz, H. Hartmann, A. Henss, C.V. Singh, D. Raabe, J. Janek, Chemo-mechanical failure mechanisms of the silicon anode in solid-state batteries, Nat. Mater. 23 (2024) 543–551, https://doi.org/10.1038/s41563-023-01792-x.
[107] Z. Wang, X. Shen, S. Chen, R. Qiao, B. Sun, J. Deng, J. Song, Large-Scale fabrication of stable silicon anode in air for sulfide solid state batteries via ionic-electronic dual conductive binder, Adv. Mater. 36 (2024) 2405025, https://doi.org/10.1002/adma.202405025.
[108] J.A. Lewis, F.J.Q. Cortes, Y. Liu, J.C. Miers, A. Verma, B.S. Vishnugopi, J. Tippens, D. Parkash, T.S. Marchese, S.Y. Han, C. Lee, P.P. Shetty, H.-W. Lee, P. Shevchenko, F.D. Carlo, C. Saldana, P.P. Mukherjee, M.T. McDowell, Linking void and interphase evolution to electrochemistry in solid-state batteries using operando X-ray tomography, Nat. Mater. 20 (2021) 5233–5239, https://doi.org/10.1038/s41563-020-00903-2.
[109] Z. Zhang, L. Wu, D. Zhou, W. Weng, X. Yao, Flexible sulfide electrolyte thin membrane with ultrahigh ionic conductivity for all-solid-state lithium batteries, Nano Lett. 21 (2021) 5233–5239, https://doi.org/10.1021/acs.nanolett.1c01344.
[110] D.J. Lee, J. Jang, J.-P. Lee, J. Wu, Y.-T. Chen, J. Holoubek, K. Yu, S.-Y. Ham, Y. Jeon, T.-H. Kim, J.B. Lee, M.-S. Song, Y.S. Meng, Z. Chen, Physio-Electrochemically durable dry-processed solid-state electrolyte films for all-solid-state batteries, Adv. Funct. Mater. 33 (2023) 2301341, https://doi.org/10.1002/adfm.202301341.
[111] G. Li, R. Xue, L. Chen, The influence of polytetrafluorethylene reduction on the capacity loss of the carbon anode for lithium ion batteries, Solid state Ion. 90 (19961) 221–225, doi:10.1016/S0167-2738(96)00367-0.
[112] D.J. Lee, Y. Jeon, J.-P. Lee, L. Zhang, K.H. Koh, F. Li, A.U. Mu, J. Wu, Y.-T. Chen, S. McNulty, W. Tang, M. Vicencio, D. Xu, J. Kim, Z. Chen, Robust interface and reduced operation pressure enabled by co-rolling dry-process for stable all-solid-state batteries, Nat. Commun. 16 (2025) 4200, https://doi.org/10.1038/s41467-025-59363-4.
[113] X. Zhao, L. Shen, N. Zhang, J. Yang, G. Liu, J. Wu, X. Yao, Stable binder boosting sulfide solid electrolyte thin membrane for all-solid-state lithium batteries, Energy Mater. Adv. 5 (2024) 0074, https://doi.org/10.34133/energymatadv.0074.
[114] Y.-J. Lee, S.-B. Hong, H.-J. Lee, H.-T. Sim, Y. Kim, S. Kim, D.-W. Kim, Flexible and thin sulfide-based solid electrolyte sheet with li^{+}-ion conductive polymer network for all-solid-state lithium-ion batteries, Chem. Eng. J. 477 (2023) 146983, https://doi.org/10.1016/j.cej.2023.146983.
[115] S.-B. Hong, Y.-R. Jang, Y.-C. Jung, W. Cho, D.-W. Kim, Sulfide-Based flexible solid electrolyte enhancing cycling performance of all-solid-state lithium batteries, ACS Appl. Energy Mater. 7 (2024) 5193–5201, https://doi.org/10.1021/acsaem.4c00547.
[116] A. Mills, S. Kalnaus, W.-Y. Tsai, Y.-F. Su, E. Williams, X. Zheng, S. Vaidyanathan, D.T. Hallinan, J. Nanda, G. Yang, Elucidating polymer binder entanglement in freestanding sulfide solid-state electrolyte membranes, ACS Energy Lett. 9 (2024) 2677–2684, https://doi.org/10.1021/acsenergylett.3c02813.
[117] S.H. Kang, J. Choi, J.Y. Kim, D.O. Shin, Y.-G. Lee, J. Lee, Mechanically robust ultrathin solid electrolyte membranes using a porous net template for all-solid-state batteries, ACS Appl. Mater. Interfaces 15 (2023) 28064–28072, https://doi.org/10.1021/acsami.3c03466.
[118] S.H. Kang, H. Lee, Y.-J. Hong, S. Myoung, H. Seo, J. Choi, S. Yoon, J.Y. Kim, D. O. Shin, M.J. Lee, Y.-S. Park, Y.-G. Lee, Y.M. Lee, High-Performance, roll-to-roll fabricated scaffold-supported solid electrolyte separator for practical all-solid-state batteries, Small 21 (2025) 2502996, https://doi.org/10.1002/smll.202502996.
[119] D.H. Kim, Y.-H. Lee, Y.B. Song, H. Kwak, S.-Y. Lee, Y.S. Jung, Thin and flexible solid electrolyte membranes with ultrahigh thermal stability derived from solution-processable li argyrodites for all-solid-state li-ion batteries, ACS Energy Lett. 5 (2020) 718–727, https://doi.org/10.1021/acsenergylett.0c00251.
[120] Y. Yan, S. Zhang, Q. Li, X. Man, X. Jiang, S. Xiong, C. Mi, Z. Zhang, C. Wang, P. Xiao, L. Yin, R. Wang, Versatile polymer-supported argyrodite-type sulfide solid electrolyte membranes for energy-dense lithium batteries, Mater. Sci. Eng. R Rep. 163 (2025) 100941, https://doi.org/10.1016/j.mser.2025.100941.
[121] X. Yang, K.R. Adair, X. Gao, X. Sun, Recent advances and perspectives on thin electrolytes for high-energy-density solid-state lithium batteries, Energy Environ. Sci. 14 (2021) 643–671, https://doi.org/10.1039/D0EE02714F.
[122] B. Emley, Y. Liang, R. Chen, C. Wu, M. Pan, Z. Fan, Y. Yao, On the quality of tape-cast thin films of sulfide electrolytes for solid-state batteries, Mater. Today Phys. 18 (2021) 100397, https://doi.org/10.1016/j.mtphys.2021.100397.
[123] Y.S. Zhang, N.E. Courtier, Z. Zhang, K. Liu, J.J. Bailey, A.M. Boyce, G. Richardson, P.R. Shearing, E. Kendrick, D.J.L. Brett, A review of lithium-ion battery electrode drying: mechanisms and metrology, Adv. Energy Mater. 12 (2022) 2102233, https://doi.org/10.1002/aenm.202102233.
[124] Y.-C. Jung, C. Hwang, M.-J. Kwak, S.-J. Jeon, Y.J. Lee, W.-J. Kwak, H.-S. Kim, K. Kim, W. Cho, J.-S. Yu, On-site formation of silver decorated carbon as an anodeless electrode for high-energy density all-solid-state batteries, J. Mater. Chem. A 11 (2023) 25275–25282, https://doi.org/10.1039/D3TA05307E.
[125] M. Dixit, C. Beamer, R. Amin, J. Shipley, R. Eklund, N. Muralidharan, L. Lindqvist, A. Fritz, R. Essehli, M. Balasubramanian, I. Belharouak, The role of isostatic pressing in large-scale production of solid-state batteries, ACS Energy Lett 9 (2024) 2677–2684, https://doi.org/10.1021/acsenergylett.2c01936.
[126] J. Cha, Y.-J. Lee, D.-W. Kim, High-performance all-solid-state lithium batteries enabled by a highly adhesive dry-processable binder, Mater. Today Energy 53 (2025) 102009, https://doi.org/10.1016/j.mtener.2025.102009.
[127] X. Li, Y. Guo, Y. Wang, J. Liu, Z. Wu, D. Wang, Physicochemical dual-force-driven PVAC@LPSCl composite electrolyte film for high-performance all-solid-state batteries, Adv. Funct. Mater. Early View e12635, doi:10.1002/adfm.202512635.
[128] V. Ponce, D.E. G.-Aranda, J.M. Seminario, Analysis of an all-solid state nanobattery using molecular dynamics simulations under an external electric field, Phys. Chem. Chem. Phys. 23 (2021) 597–606, https://doi.org/10.1039/D0CP02851G.